Modern fluid motion physics: on the jet streams induced by a body form in the unrestricted uniform flow of real fluid. Part 1: the thin flat plate

S.L. Arsenjev[1]
Physical-Technical Group
Dobroljubova Street, 2, 29, Pavlograd Town, Dniepropetrovsk region, 51400 Ukraine

Analysis of the results of the well-known experimental researches carried out at the first third of XX century allowed for the first time to create the rational conceptual model of the flow kinematics and the interaction dynamics of the unrestricted uniform flow of real continuous medium – mainly air – with a solid body. The body is presented in a kind of the thin flat plate of the infinite span at any angle of attack. Unity of fields of the flow trajectories and velocities with the force field of the flow action onto the body is achieved by means of orthogonal conjugation of curves from assemblage of conical sections – circumference, ellipse, parabola, hyperbola – in combination with the local continuity condition and with introducing a conception on the jet streams induced by interaction of the body form with the unrestricted flow part running immediately against the body. Forces of viscosity act in accordance with the boundary layer theory in internal and external boundaries of these jet streams. Concrete examples of graphical construction and corresponding calculations show the method of determination of the pressure and rarefaction distribution on the body front and back sides and interaction of these forces between its.
PACS: 43.40.-r; 43.40.Cw; 43.40.Dx; 47.10.+g; 47.15.-x; 47.27.-i; 47.27.Vf; 47.27.Wg; 47.32.Cc; 47.32.Ff; 47.85.-g; 47.85.Dh; 47.85.Gj; 47.85.Kn; 47.85.Np

Introduction

A subject of study in the given article is a problem on mechanics of interaction of unrestricted uniform flow of real fluid, mainly air, with a solid body. In utilitarian interpretation, the problem comes to determination of resistance what the fluid flow exerts to the body moving in it.
In his fundamental work [1] I. Newton for the first time has produced above-mentioned resistance in the kind of a sum of three components: a force of adhesion of a fluid to a body surface, a force of friction of the fluid layers relatively each other and a force of blows of the fluid ponderable particles onto the front part. Supposing the third of the enumerated components as sole considerable part of the resistance, Newton has supposed that a quantity of the resistance depends on: a size of the body cross-section (middle) area, subjected to the blows of the unrestricted uniform flow particles what run immediately against the body, irrespective of the body form, the body motion velocity and the fluid density. At the same time Newton was supposing that a pressure in the flow behind the body is equal to the pressure in the flow far from the body. According to such approach, a ship, having small resistance, can be long, but one must without fail be narrow and shallow-draught. Effectiveness of these recommendations has received the most striking corroboration in a design of the sporting row-boat called by academic eight-boat. These boats ~10 m long, ~0.54 m width and ~0.145 m draught are used by students of Cambridge and Oxford Universities at its yearly contests since the second half XVIII century up to now.
French military engineer P.L.G. Du Buat (1764), in his experiments with a flat box furnished with small orifices and submerged vertically into water stream across flow, has detected that the water pressure onto the box front wall is higher than atmospheric one and the water pressure onto the box back wall is lower atmospheric pressure [2]. French engineer G. Eiffel (1912) – constructor of the illustrious lattice tower in Paris, – in his experiments with the flat plates

[1] Phone: +380993630224 (Rus.)
E-mail: usp777@ukr.net, ptglecus37@yahoo.co.uk

submerged vertically into the water stream at an angle to the flow direction, had detected [2] that the force created by rarefaction behind the plate is much more the pressure force on its front side. English investigators A. Fage and F.C. Johansen (1927), in his experiments with the flat plate submerged into the air stream across flow at its different incidence, had taken the pressure distribution on its front and back sides [3], and thereby they had quantitatively confirmed the experimental results of Du Buat and Eiffel.

In parallel to experimental investigation of action of the air and water flow onto flat plate, analogous experiments were conducting with bodies in the kind of circular cylinder and ball. Eiffel (1912) and then [4] L. Prandtl (1914) were determining resistance of a ball in air stream. O. Flachsbart (1927) had experimentally determined the air stream pressure onto the ball in its diametrical – longitudinal – section [5]. Flachsbart (1932) had also experimentally determined the air pressure distribution along the circumference of a cylinder cross-section [5], and American investigator D. Meksyn (1961) had experimentally determined [6] the air stream maximum velocity nearby the cylinder surface; the velocity, in a section at angle of 70 degrees from frontal critical point, exceeds by 1.6 time velocity far from the cylinder. (Owing to developed experimental base, the similar experiments are also conducted and now).

Special attention to experimental investigation of interaction of the real fluid flow with the thin flat plate, circular and elliptical cylinders and ball is stipulated by that these bodies present by itself formative elements of compound structures of the overland, water, and air transport and facilities (fluidics, pneumatics, pneumonic…). But in contrast to cylinder and ball, the thin flat plate is the simplest in its form body. By means of the plate one can separately and jointly investigate experimentally the friction resistance and the form drag by means of simple changing of its orientation (incidence) in the real fluid flow. The results of such experiments create possibility for fruitful development of conceptual physical model. But and now, the numerous applied problems of aero- and hydrodynamics are solved by means of experiment in the numerous model testing basins, the wind and water tunnels with the scaled and full-scale models for determining of dimensionless quantities of drag (C_d), lift (C_l) and other coefficients.

Adducing in his monograph [7] brief survey of the aero- and hydrodynamics modern state, N.V.Kokshaysky (1974) was writing: "*In the applied hydromechanics these coefficients have a salient meaning as, in the end, just the ones answer for all those physical features influencing on the drag and lift, which ones are difficultly or impossibly to state by simple analytic expressions and which ones are bound up with the body form, its orientation in the stream, quantity of Reynolds number*."

Development of the theoretical aero- and hydrodynamics in the second half of XX century was accompanied by the following statements.

H. Schlichting (1965): "*…the theory of ideal fluid is quite powerless for solution of problem on the resistance calculation of a body moved in* (real – the author's note) *fluid*" [6].

S. Goldstein (1943): "*Mathematical calculations by means of the boundary layer theory are based on the pressure distribution given beforehand. The boundary layer theory not allows to determine the distribution*" [8].

M.I. Gurevitch (1961): "*…the jet theory (of ideal fluid – the author's note) cannot give the total picture of the air flow around a plate and a cylinder. The jet theory not allows also getting a pressure behind the body*" [9].

M.A. Lavrentjev (1977): "*…reserve of harmonic functions is so great, that a looking-for of that of ones, which is answering to the problem condition, is generally difficult*," and "*…with theoretical point of view, dimensional method has not led to success*" [10].

After interpretation by M.V. Morkovin (1964) of the formation features of the attached and free vortexes [11], S.M. Bjelotserkovsky and all (1988) have adduced a description of a numerical "method of the discrete vortexes" and some results obtained by means of the computer calculation [12]. According to the method, a flow around a body is divided onto two zones: the viscous flow in the boundary layer near the body surface and ideal flow in surroundings.

Although the book is dedicated to the flow separation and although the flow separation on both

sides of plate is long ago shown in fig.83 in the well-known book [3], the results of such computer calculation are not adduced by the authors.
The aim of the given article is an elucidation of mechanics of interaction of the thin flat plate with the unrestricted uniform air flow.

Approach
According to the aim raised in the Introduction, the approach to the problem solution is based on application of so called Physical Ensemble method devised and verified by the author in the process of solution of a number of previous problems [13]. In particular, conformably to the problem, the method envisages:
- creating of general conceptual model of the flow and the plate interaction;
- elucidating of geometrical structure of the flow field;
- determining of the kinematics parameters of the flow around the plate;
- determining of the interaction dynamics of the flow with the plate;
- creating of the conjugated graphical and analytical description allowing to consider a variety of the interaction variants of the flow and the plate from single position.

The results of experimental research, adduced in [3, fig. 83], are used as initial data and for comparison with the results of the given research. Application of graphic-analytical method is stipulated by the following two circumstances: firstly, effectiveness of combination of geometrical constructing with its analytical description surpasses effectiveness of every of these methods taken separately and, secondly, the combination provides high explanatory function.

Solution: part 1
1. The simplest case, when the body form only exerts influence upon structure of the motion field of the unrestricted uniform flow of real fluid (in the given case – air), is realized by means of the thin flat plate $2b$ width, with its unrestricted span and oriented strictly across the flow.
Preliminary analysis of the flow field around the plate allows, in the frameworks of creation of the general conceptual model, to distinguish the following parts of the flow:
- one part of the flow, in the limits of the plate width, running immediately against the plate front side – the flow part before obstacle;
- two parts of the flow passing by the plate and touching its edges;
- one part of the flow, in the limits of the plate width, adjoining immediately to the plate back side (so called dead water) – the flow part behind obstacle.

The first of enumerated parts of the flow is divided onto two the same streams and every of them turns to the nearest edge of the plate for passing by the obstacle. In that way the flow part is transmuted into two jet streams. These jet streams form a brake zone between itself and the plate front side. In the zone, a profile of distribution of the surplus (dynamical) pressure corresponds to a curvature of internal boundaries of the jet streams, as it is shown in the previous article [13, fig. 2a] of the author. Two flow parts passing by the plate exert lateral resistance to pushing on these jet streams. Such action of external passing flow leads to narrowing of cross-section of the jet streams and to a corresponding increase of velocity and a velocity head of the jet streams. As a result, the jet streams overcome the lateral resistance of external passing flow and flow round the plate driving away the external flow. Just the jet streams determine, in the main, implementation of the local and general continuity condition when the unrestricted flow goes rounds an obstacle. Moving with outstripping of the external passing flow and having its velocity head considerably greater than the latter, the jet streams surround the flow part behind the plate and exert onto it the ejector action.
At low velocities (low Reynolds numbers) of the unrestricted flow, the jet streams form a closed pair-vortex structure behind the plate. An interaction of every of two jet streams with the vortex induced by its action has two consequences: on the one hand, a linear velocity of rotation of the vortexes is approximately equal to the jet velocity, on the other hand, the jet by its velocity head carries along follow it, and correspondingly away from the plate, all mass of the vortex structure

and thereby creates quite uniform rarefaction at the plate back side. An absolute quantity of the rarefaction is equal to the jet velocity head. In that way the surplus pressure onto the plate front side and the rarefaction at the plate back side constitute together the total force of action of the real fluid flow onto the thin flat plate submerged in it strictly across. A correlation of the total force components is the following:

- a maximum quantity of the surplus pressure onto the plate front side is determined by a velocity head of the unrestricted flow; the pressure distribution along the plate profile is approximately similar to a semi-circumference or semi-ellipse;
- a maximum quantity of the rarefaction behind the plate is determined by the velocity head of the jet streams induced by interaction of the body form with the real fluid flow; the rarefaction distribution along the plate profile is uniform.

Approximate qualitative appraisal of the correlation of the total force components allows supposing that the force, stipulated by the rarefaction behind the plate, is no less two times more the force acting onto the plate front side.

At high velocities (high Reynolds numbers) of the unrestricted flow, it is going on the qualitative alteration in interaction of the jet streams with the flow part behind the plate. Now every of the jet streams can self-dependently draw in the vortex motion the whole of the flow part adjoining immediately to the plate back side. Now formation of the vortexes is going on by every of two jet streams separately. A completion of formation of a vortex by one jet leads to formation of a new vortex by other jet. A growth of the vortex formed by the second jet promotes a throwing out of the vortex formed by the first jet. A frequency of throwing out of the vortexes out of zone behind the plate is in direct proportion to the flow velocity and in inverse proportion to the body size and one also is bound with Strouhal number (1878) and Reynolds number (1883).

The growing (increasing) vortex formed by the second jet stream throws out the developed vortex formed by the first jet stream across the unrestricted flow by its centrifugal force. As a result the first vortex goes out from aerodynamic shad of the plate and undergoes to a direct action of a velocity head of the first jet stream in direction of the unrestricted flow. In this transitory period, an interaction of the first vortex, reached its maximum size and mass, with the first jet stream is accompanied by sharp deflection of the first jet stream in a side away from the plate edge across the unrestricted flow and leads to the partial separation of the first jet stream away from the plate front surface near its edge. As it is shown in [3, fig. 83], the separation length reaches a quarter of the plate profile at its attack angle 15^0 is reached. The cyclical throwing out of the vortexes by turns away from every of the plate edges leads to the cyclical warp of the rarefaction uniform distribution behind the plate and, as consequence, leads to an origin of the alternating forces even in quite symmetrical system of the plate and flow interaction. Naturally, the above-descripted mechanics can be realized only owing to the fluid internal friction, i.e. to its viscosity.

A description of interaction of the jet streams and vortexes induced by the streams with two parts of the unrestricted flow passing by the plate comes to the following:

- the jet streams increase its velocity as ones approach the plate and ones drive away the parts of the flow away from the plate edges, i.e. a velocity of the jet streams is equal to or more than the flow velocity;
- a velocity of a mass center of the vortexes is commensurable with the flow velocity, but a linear velocity of the vortex rotation is similar to a velocity of the jet streams.

In that way both - an average velocity of the jet streams and a linear velocity of the vortex rotation - exceed the unrestricted flow velocity.

The above-stated description in a qualitative aspect of the interaction phenomenon of the flow with the plate submerged across the flow is description of the general conceptual model as the necessary condition for transition to the following problems on kinematics and dynamics of the flow field around the plate at different angles of attack in the limits of $90° \geq \alpha \geq 0$. Naturally, the case $\alpha = 90^0$ is considered as the first of these problems.

Going consequently from the simple to the complex, the author supposes advisable to use in the beginning the solutions stated in his previous article [13, fig. 2a] to elucidate the question on kinematics of the flow before the plate in the limits of its width.
Fig. 1(a, b) shows two combined geometrical diagrams of interaction of the liquid free jet with the plate. The left side of these two diagrams shows, for a comparison, the above-mentioned solution [13, fig. 2a], and fig. 1a, in its right side, represents the possible geometrical construction of the jet running against the plate under condition of equality of the plate width to the flat jet thickness. Fig. 1b, in its right side, shows other geometrically possible construction. In spite of its geometrical possibility, these latter two diagrams not allow to achieve a compatibility with the passing lateral flow. Apparently, the geometrical constructions by means of the circumference arches are too simple and ones cannot be used as a base for geometrical solution of the problem on interaction of the plate with the unrestricted flow. At the same time the co-ordinate net of the diagrams in fig. 1a, b determines the spatial location and the scale of the plate half width – in the right side of the diagrams – relatively to the horizontal basic flatness line, BFL90, passing through the plate profile in which the liquid free flat jet is turning at an angle 90° (at the left). A distance from the horizontal basic flatness line, BFL90, up to the plate profile (at the right) is $h_{90} = b_{90}/4$. Here and further in the given article, the numerical scripts and subscripts will be indicate the plate attack angle.
Further subsequent solution of the problem is based on a use of the curves from assemblage of conical sections: an ellipse, a parabola, a hyperbola and a circumference with its evolvent.
Fig. 2a, in its right side, shows a construction of equilateral hyperbola strictly passing through the plate edge. Physically real part of the hyperbola is separated from its full geometrical construction by the plate edge. The real part of the hyperbola is the effective internal boundary of one of the two jet streams induced by the plate in the unrestricted flow part running immediately against the obstacle. The same hyperbola, in the given case, determines also a profile of dynamical pressure of the jet stream onto the plate front side. Method of construction of the pressure profile is shown in previous article of the author [13, fig. 2a]. A constructing of trajectories of the slow motion in a zone between the flow axis, the plate profile and the internal boundary of the jet stream (in the kind of hyperbola constructed) is shown in the right side of fig. 2b by means of three small circumferences with its centers in a straight line at an angle of 45° from a point of intersection of the flow axis with a middle of the plate profile. These circumferences determine the tops of the equilateral hyperbolas in zone of the slow motion.
Fig. 3 shows a constructing of external boundary of the jet stream considered. This is a boundary of a contact interaction of the jet stream with the external passing flow. The boundary is also equilateral hyperbola; a succession of its construction is the following:
- a circumference with its radius equal to $r_{90} = b_{90}/\sqrt{2}$ (in fig. 2a, the top of the hyperbola) is displaced up to a coincidence of its center with the plate edge;
- the radius r_{90} at an angle of 45° to the flow direction indicates a point of a smooth contact of the hyperbola with the circumference;
- the hyperbola asymptotes are two reciprocally perpendicular straight lines in the kind of the BFL90 and a line passing through the plate edge;
-the radius r_{90} restricts the physically real part of the hyperbola from its full geometrical construction; the real part of the hyperbola is effective external boundary of one of the two jet streams induced by the plate in the unrestricted flow part running immediately against it.
The points of a beginning and an end of the radius r_{90} are used to construct a secant parabola (or a secant ellipse) with the BFL90 as its symmetry axis. A control point of the secant parabola construction is $x = y = b_{90}$. The real part of the secant parabola - over a line coinciding with the plate profile – is orthogonal to the internal and external effective boundaries of the jet stream, and one allows constructing the intermediate hyperbolic lines both in the limits between the internal and external boundaries of the jet streams and outside the limits. The secant parabola is used for a secluded plate in the unrestricted flow, and the secant ellipse is used in the presence in close vicinity other plate in a flatness of the first one. The symmetry axis of these curves – the

secant parabola or ellipse – remains always by perpendicular to the unrestricted flow direction; the real part of every of these curves remains by orthogonal to the internal boundary of the jet stream at any incidence of the plate. As a result of such construction, a cross-section area of the jet stream is determined by a quantity of r_{90} is $A_j = b_{90}^2/\sqrt{2}$ and, accordingly, an average velocity of the jet stream in the cross-section is $v_j = v_0\sqrt{2}$. These parameters of the jet stream answer $Q_0 = Q_j$ as the continuity condition, where

$$Q_0 = v_0 A_{90} = v_0 b_{90}^2 \quad (1)$$

$$Q_j = v_j A_j = v_0\sqrt{2}\, b_{90}^2/\sqrt{2} = v_0\, b_{90}^2; \quad (2)$$

and on the other hand these parameters signify

$$\rho v_j^2/2 = 2\,\rho v_0^2/2, \quad (3)$$

i.e. ability of the jet stream to force its way through between the plate edge and the unrestricted flow parts passing by the plate.

The considered case corresponds to the subsonic air flow, $v_0 < 0.65\sqrt{kgRT}$, when the air density is invariable, $\rho_j = \rho_0$, and thus the case corresponds also to the water flow.

The accelerated motion of the jet stream up to the secant parabola is accompanied by some losses on its internal and external boundaries. The smooth increase of a thickness of the boundary layer, forming a braking zone before the plate up to a quantity commensurable with a thickness of the jet stream itself, is bound with negligible losses stipulated by the fluid internal friction. The smooth increase of the jet stream velocity relatively to the unrestricted flow part passing by the plate is also not bound with significant losses stipulated by the fluid internal friction as a difference of velocities in this boundary cannot exceed $(v_j - v_0)/v_0 < 41\%$.

The maximum quantity of hydraulic losses of the jet stream is bound with its acceleration and with corresponding relative decreasing of its cross-section area; these losses, according to the known in hydraulics reference data, not exceed approximately 8% for $A_j/A_0 \cong 0.71$.

Further motion of the jet streams behind the secant parabola arch passes smoothly in parabolic (elliptic) trajectory with further some increase of its velocity and, correspondingly, velocity head at sufficiently high velocity of adjacent layers of the unrestricted flow.

As to a kinematics of the unrestricted flow field outside the external boundary of the jet streams, its geometrical structure is quite similar to a construction of external boundaries of the jet streams in combination with successive increase of a curvature radius in a top of the hyperbolas, with corresponding successive increase of the parabolas continuing the hyperbolas as well with maintenance of orthogonal conjugation of these curves relatively to the secant parabola arch. Such simple construction is quite sufficiently, as just the jet streams, induced by the body form in the unrestricted flow of real fluid, determine a kinematics of the flow field around the body and dynamics of its interaction, including a determination of the body drag, lift, moment. In the other words: the near flow field, formed by the jet streams around the body, determines as a whole kinematics and dynamics of interaction of the body with the flow. And the flow outside the near field is a medium as far as disturbed kinematic as much as compensated dynamic. The above-stated description of geometrical construction of the far field kinematics ensures a gradual degeneration of its curvilinear structure into the undisturbed unrestricted flow of the real fluid.

Going by the plate, the jet streams come into interaction with the flow part behind the plate. At sufficiently low velocity of the flow, when forces of the fluid inertia and its viscosity are commensurable, the jet streams turn round the plate edges and run symmetrically against each other immediately near the plate back side. Such jet streams form very weak rarefaction behind the plate and ones turn reciprocally and move down flow without formation of vortexes.

The some increase of the flow velocity is accompanied by formation of the symmetrical closed pair-vortex structure between the jet streams and the plate back side. As the flow velocity increases, it is going on an increase of dimensions of the pair-vortex structure up to its maximum state: its form is an oval with its minor axis about $\sim 1.5 \cdot 2b_{90}$ and its major axis (along the flow) about$\sim 2.3 \cdot 2b_{90}$, and the state is accompanied by oscillations in the kind of the mutual-alternate increase and decrease of every of the two vortexes in its pair.
Further increase of the flow velocity is accompanied by the sweeping change of interaction of the jet stream with the flow part located behind the plate: now a velocity head of every of the two jet streams is sufficient to involve at once the whole of the flow part located behind the plate into rotational motion. Now the practically whole of a force of every of the two jet streams

$$P_{jp} = A_{jp}\ \rho v_{jp}^2/2 > A_{90}\,\rho v_0^2, \tag{4}$$

where $A_{jp} = A_j/1.08$ is a cross-section area of the jet stream with its center in the plate flatness; v_{jp} is an average velocity of the jet stream in the same place, $v_{jp} = 1.08v_0^2\sqrt{2}$, - acts tangentially onto the fluid mass adjoining to the plate back side and one rolls up the mass into vortex. At the same time the force, P_{jp}, acts, in accordance with mechanics law, also onto the vortex mass center and pushes away the vortex from the plate, down flow. An increase of the vortex diameter, as its development, leads to its interaction with the jet stream coming down from the plate opposite edge. A result of the interaction is a development of a new vortex having its rotation concordant with the first vortex. The new vortex, as its development, displaces the first vortex to the first jet stream. A joint action of the longitudinal force of the first jet stream and the transversal force of the new – developing – vortex leads to pushing off the first vortex away from the plate. In the transitory period of the pushing off, the first vortex crosses the first jet stream. As a result, the first jet stream moves sharp aside up to separation from the plate front side near its edge. The diagram in [3, fig. 83] shows the separation in the kind of a lack of coincidence of the plate profile width and of the pressure profile width in the plate profile. The diagrams in the above-mentioned figure show simultaneous separation near both edges of the plate. Such picture is a consequence of using of the device for the pressure measurement with its frequency lower than frequency of periodical formation and pushing off the vortexes by turn away from the plate edges. Uniformity of the rarefaction profile behind the plate, shown in the same figure, also not correspond to reality because of the same cause. At the same time periodic pushing off the vortexes is a source of the moment alternating loads in addition to the drag.
As a whole, just the force (4) of the jet streams, induced by the body form, determines degree of rarefaction behind the plate at the developed aero- and hydrodynamic interaction of the flow and the plate. Average in time quantity of rarefaction behind the plate is determined by means of expressions (1, 2 and 3)

$$p_{90} = -\left(A_j/A_{90}\right)2\rho\, v_0^2/2 = -\rho\, v_0^2/\sqrt{2} \cong -0.7\rho v_0^2. \tag{5}$$

Such result corresponds quite to the results of experimental research obtained by Fage and Johansen, adduced by Goldstein in his book [8].
The same correspondence can be got by a summation of absolute quantities of the maximum pressure on the plate front side and rarefaction at the plate back side at $\alpha = 90^0$, taken from the first diagram in [3, fig. 83]. Hence a quantity of the drag coefficient of the plate – with approximate regard for a curvature of the pressure distribution on the plate front side – is

$$C_D' \cong \pi/4 + \sqrt{2} \cong 2.2, \tag{6 a}$$

and with taking into account of ~8% hydraulic losses, bound with a narrowing of a cross-section of the jet streams at its acceleration up to $1.41v_0$, the drag coefficient is approximate

$$C_D \cong C_D'(\ 1 - 0.08) \cong 2.02. \qquad (6\ b)$$

A use of the jet streams of a gas and liquid to a creation of rarefaction is well-known as ejection. Now, completing the problem solution on interaction of the unrestricted flow of the real fluid with the plate submerged into it across flow, the author supposes that a question on difference of nature of the form resistance in contrast to the resistance stipulated by the fluid internal friction is sufficiently elucidated. These both types of resistance can be demonstrated in separate by means of the same thin flat plate submerged into the unrestricted flow along or across the flow direction. In the first of these two cases, a resistance is basically stipulated by physical property of the real fluid to transfer a momentum of each its layer to the other, by adhesion to the body surface and by the surface roughness; the trajectories of the uniform flow field remain almost immutable near the body surface. In contrast to it, the body form is the obstacle on a way of the unrestricted flow of the real fluid. A property of the real fluid in the kind of its internal motion freedom owing to a mobility of its particles ensures a possibility for passing by the obstacle as a necessary condition for a flow. And a sufficient condition, realizing the possibility into a reality, is the first law of hydraulics as the continuity condition. Naturally, the problem solution on passing by obstacle under these two conditions is realized by that part of the unrestricted flow which one runs immediately against obstacle. A result of the problem solution is formation of the jet streams determining the body drag, lift and so forth.

2. An elucidation of a nature of the body form resistance and solution of the problem on kinematics and dynamics of interaction of the unrestricted flow of real fluid with the plate submerged into it across flow allows to go on to the problem solution on interaction of the same flow with the same plate at any angles of attack .

A solution of the problem is expediently to begin from a short description of general signs and some features of interaction of the unrestricted air flow with the plate at some angles of attack, what can be marked by looking at the diagrams in fig. 4 and fig. 5 constructed by means of the diagrams in [3, fig. 83]. Judging from the pressure profile on the front and back sides of the plate, it appears possible to mark out three groups of the attack angles. Between these groups, it should be supposed qualitative differences in kinematics and dynamics of interaction of the flow with the plate.

In particular, distinctive signs in the first group, in the $90^0 \geq \alpha \geq 15^0$ limits, are the followings:

- a quantity of maximum pressure of the flow onto the plate front side remains invariable in spite of sufficiently considerable change of the attack angle;
- a point of action of the flow maximum pressure onto the plate front side is displaced smoothly from the plate profile middle at $\alpha = 90^0$ to its front edge at $\alpha = 15^0$;
- the rarefaction distribution on the plate back side remains approximately uniform along the plate profile;
- a quantity of rarefaction behind the plate is decreased accordingly to the law very similar to sinusoidal and at $\alpha = 15^0$ one is decreased twice in comparison with its quantity at $\alpha = 90^0$;
- periodical separation of the jet stream from the plate front side near its front edge is stopped at $\alpha \cong 70^0$, and the separation length near its rear edge is increase smoothly up to a quarter of the plate profile, at $\alpha = 15^0$.

Distinctive signs of the second group in the limits of $6^0 \geq \alpha \geq 0$ can be as the followings:

- a quantity of maximum pressure, on the front edge of the plate front side, has been decreased approximately by 5% at $\alpha = 6^0$ in comparison with its quantity in the first group, and quantity of rarefaction – also on the front edge but of the plate back side – has been increased approximately by 30% at $\alpha = 6^0$ in comparison with its quantity at $\alpha = 15^0$;
- the pressure profile on the plate front side is very concave and on the plate back side is concavo-convex;
- it should be supposed that a further decrease of the attack angle up to $\alpha = 0$ leads to sufficiently smooth degeneration of the dynamical pressure and rarefaction profile on the plate surfaces and to a transition of dependence of the plate drag only on the fluid viscous forces;

length of zone of the flow separation from the plate back side is shortening and thickness of the flow part before and behind the plate disappears as the attack angle is decreasing up to zero.
The results of experimental research in the intermediate group, at the attack angles in the limits of $15^0 \geq \alpha \geq 6^0$, are not adduced in the above-mentioned diagram [3, fig. 83]. But it may be supposed that this is a group of transitional processes, in which the long vortex wake behind the plate, in the first group, is shortened up to the plate width in the second group.
Judging from reference to [3, fig. 83], the experiments had been conducted with a use of the air flow. Judging from the pressure and rarefaction distribution form, an increase of the separation length of the jet stream from the plate front side near its rear edge, having as before cyclical nature, is stipulated by approach of the plate incidence to the passing flow direction as the attack angle is decreased in the limits of $90^0 \geq \alpha \geq 15^0$.
The above-stated description of the general signs and the separate features allows, in the author view, to reproduce a kinematics of the near field of the flow around the plate and the pressure distribution on both sides of the plate by graphic-analytical method.
Fig. 5a shows the combined circular diagram constructed by superposition through 15^0 of the plate profiles and by circumscribing of these profiles by a goniometrical circle. The left lower quarter of the circle contains the circumference evolvent arch crossing the plate profiles in the $90^0 \geq \alpha \geq 15^0$ limits. A point of a beginning of the evolvent arch is joined with the rear edge of the plate profile at $\alpha = 6^0$ by the slightly bent line. The radial distance between the goniometrical circle and the evolvent arch indicates a maximum length of the periodical separation of the jet stream from the plate front side near its rear edge. The intermittent separation of the jet stream from the plate front side near every of its edges at $90^0 \geq \alpha \geq 70^0$ is shown by two not great arches, one of which – at the left – is joined with the evolvent arch. A decrease of the attack angle from 15^0 up to 6^0 is accompanied by sharp shortening of the periodical separation zone of the jet stream from the plate front side near its rear edge and by the same sharp shortening of the long vortex wake behind the plate up to the plate width as well by transmutation of the vortex wake into the local separation zone in the limits of the plate profile.
Fig. 5b, in the right upper quarter of the goniometrical circle, contains a semi-circumference with its diameter equal to the goniometrical circle radius. The semi-circumference is displaced to the right just up to an intersection of its arch with a circumference of the goniometrical circle in a point placed in the circle at $\alpha = 15^0$ angle. The points of intersection of the plate profile with the semi-circumference indicate a position of the bifurcation line of the jet streams, BLJ, on the plate front side at the $90^0 \geq \alpha \geq 15^0$ attack angles. The line is a hyperbola with its asymptotes in the kind of a straight line coinciding with upright diameter of the goniometrical circle, as the general asymptote at any angles of attack of the plate, and a straight line from center of the goniometrical circle at the doubled angle of attack clockwise from the general asymptote; the plate profile is the symmetry axis of the hyperbola. A combination of two asymptotes, of the symmetry axis and the point indicating, in the given case, an apex is the necessary and sufficient conditions of geometrically right and correct construction of the hyperbola. A real part of the hyperbola is placed before the plate profile and one is limited by its apex. The other part of the hyperbola, behind the plate profile, has not a physical sense. The hyperbola is straightened into a straight line and coincides with upright diameter of the goniometrical circle when the attack angle $\alpha = 90^0$ is reached.
In the same quarter, the base flatness lines, BFL, accompany the every plate profile locating parallel to and behind it. These lines, BFL, form a geometrical fan similar the fan formed by the plate profiles. A center of the fan is displaced below from a center of the goniometrical circle on $h_{90} = b_{90}/4$ distance. This initial distance is decreased as the attack angle is decreased according to $h(\alpha) = h_{90} \sin \alpha$ dependence. The straight lines perpendicular to every BFL and passing through the points of intersection of the plate profile with the above semi-circumference are asymptotes of two equilateral hyperbolas determining the pressure distribution of the flow onto the plate front side. Method of construction of the pressure profile will be stated below.
The radii - r_{90}, r_{75}, r_{60}, …, (subscripts are bound with the plate attack angle) - determine the

effective thickness of the jet streams at both edges of the plate and ones are always oriented at 45^0 angle only to the flow direction. A quantity of the radii is decreased as the attack angle is decreased corresponding to $r(\alpha) = \left(b_{90}/\sqrt{2}\right)\sin\alpha$ dependence. The dependence is graphically expressed by two elliptical arches passing through a free end of the every radius.
It can be noticed that an angle between the radius and the plate profile, at its front edge (in the right upper quarter), is increased as the attack angle is decreased and in contrast to it an angle between the radius and the plate profile, at its rear edge (in the left lower quarter), is decreased as the attack angle is decreased up to $\alpha = 15^0$. In the first of these two cases, an increase of the angle intensifies counteraction to a separation of the jet stream from the plate front surface at its front edge. In the second case, a decrease of the angle promotes separation of the jet stream from the plate front surface at its rear edge. In the latter case, the separation of the jet stream is stipulated by action of three factors: an effective thickness, r, of the jet stream near the plate rear edge, a scale of the vortex pushed away from the plate and the angle between the radius and the plate profile. The first two factors are decreased as the attack angle is decreased. The transitory action ($\alpha = 90^0$) of the large-scaled vortex leads to a deflection of the radius r_{90} by an angle about 50^0 and one provokes a not great separation of the jet stream from the plate front side by turns near its every edge. An action of the reduced to fragments vortexes ($\alpha = 15^0$) is very relaxed although the effective thickness of the jet stream is also considerably decreased. A quantity of the separation, stipulated by action of combination of these two factors, is shown in the left lower quarter in fig. 5a in the kind of a circumference arch going close by and equidistant to the goniometrical circle in $90^0 \geq \alpha \geq 15^0$ limits. The rest of the length part of the separation zone, between the circumference arch and the evolvent arch, is stipulated by smooth decrease of an angle between the radius and the plate profile from 135^0 ($\alpha = 90^0$) up to 60^0 ($\alpha = 15^0$).
Fig. 5c: at the different attack angles, the graphical constructing of the flow field trajectories presupposes also a use of the secant parabolas localized at the plate edges. As before (see fig. 3), the symmetry axes of these curves remain perpendicular to the undisturbed flow direction, and its dimensions – axial length and chord – are decreased simultaneous on dependences:
$l(\alpha) = l_{90}\sin\alpha = 2b_{90}\sin\alpha$ and $c(\alpha) = c_{90}\sin\alpha = 2.5b_{90}\sin\alpha$.
These curves have a property to a jumping forward – against the flow direction – in transitory periods of a pushing off the vortexes away from the plate back side. For example ($\alpha = 90^0$), these parabolas jump forward and thereby ones provoke comparatively not great separation of the jet stream near edges of the plate front side as it is shown in fig. 5a from the left and right of the goniometrical circle. The right parabola discontinues the jumping at the attack angles less 70^0, and the left parabola continues the jumping up to 15^0, when a length of the jet stream separation from the plate rear edge riches about quarter of the plate profile length. In the $90^0 \geq \alpha \geq 0$ limits, a decrease of rarefaction behind the plate is bound with a decrease of thickness of the jet streams according to $A_j(\alpha) = A_{j90}\sin\alpha$ dependence.
The special explanation is demanded for the below following situation. A maximum quantity of dynamical pressure onto the plate front side, according to [3, fig. 83], is displaced from the plate profile middle to its front edge as the attack angle is decreased from $\alpha = 90^0$ up to $\alpha = 15^0$, and at the same time the quantity remains constant and equal to the doubled velocity head, ρv^2. Such combination of properties of the dynamical pressure is evidence to an action of the pressure along the normal to the plate profile. At the same time, according to the fig. 83 [3], a maximum quantity of the dynamical pressure onto the front edge of the plate is approximately 95% at the attack angle $\alpha = 6^0$ in a comparison with the quantity when the attack angle is in the limits of $90^0 \geq \alpha \geq 15^0$. Physical aspect of the situation at $\alpha = 6^0$ is in the following:
- on the one hand the maximum velocity head of the flow part running immediately against the plate remains invariable when the attack angle is $90^0 \geq \alpha \geq 15^0$ in the limits;
- on the other hand a decrease of the attack angle from 15^0 up to zero ought to be accompanied by a corresponding decrease of the maximum dynamical pressure onto the plate also up to zero.

A reasonable way out from the situation is in the following supposition: a vector of the flow velocity head ought to be deflected from a normal to the plate profile up to its coincidence with the plate profile when its attack angle equals a zero. The deflection of the vector ought to accompany by a decrease of its quantity according to $P_V(\varphi) = p_{max}(\varphi) = \rho v_0^2 \cos\varphi$, where φ is an angle between the plate normal and the vector deflected.

Fig. 6 shows that such deflection is quite possible, when the deflection begins from $\alpha = 9^0$ and drag of the plate disappears at $\alpha = 0$. At the same time, it is offered by possible to determine the maximum pressure onto the plate front side in its front edge at $\alpha = 6^0$. According to the table in fig. 6, the quantity $p_{max} = \rho v_0^2 \cos 16^0 = 0.96\rho v_0^2$ practically coincides with the above-mentioned result of experimental research. It should be noted the following: a quantity of the vector, determined by the angle cosine of its deflection from the normal to the plate profile, is a quantity of the maximum pressure, acting along the normal to the plate profile. In other words: a quantity of the maximum pressure, acting as before along the normal to the plate profile, is decreased according to $\cos\varphi$ from $\alpha = 9^0$ up to zero.

The line of the flow bifurcation, BLJ, into the two jet streams, at the attack angles in the limits of $8^0 \geq \alpha \geq 0$, also represents by itself a hyperbola. But in contrast to the limits of $90^0 \geq \alpha \geq 9^0$, where the hyperbolic line, BLJ, was divided by the plate profile into two equal parts, these hyperbolic lines rest against the plate front edge. A constructing of these lines is quite similar to that at $90^0 \geq \alpha \geq 9^0$ limits. But now the hyperbola at $\alpha = 9^0$ is used for the plate at $\alpha = 8^0$, and the hyperbola at $\alpha = 8^0$ is used for the plate at $\alpha = 7^0$ and so on. Such constructing presupposes a successive displacement of every hyperbola along the flow direction up to its smooth contact with the subsequent vector and at the same time up to the rest against the plate front edge. Branches of these hyperbolas draw together as the attack angle is decreased from 9^0 up to zero, when the branches of the last hyperbola are joined into a single straight line. In that way a width of the flow part running immediately against the plate becomes equal to zero and, according to it, the jet streams and the form resistance of the plate almost disappear.

Elucidation of an influence of the vortexes pushed off away from the plate rear edge onto the jet stream separation from the plate front side allows also to explain a cause of origin of a straightening and then of an increase of concavity of the pressure distribution curves on the plate front side near its rear edge shown in fig. 83 [3]. A smooth moving away of the evolvent from the goniometrical circle, in fig. 5a, signifies not only an increase of the separation zone length on the plate front side, as the attack angle is decreased, but also an increase of the deflection angle of the jet stream in the separation point. As a result of it, the jet stream already before the separation point turns about more sharply from the plate surface and one stipulates thereby the above-mentioned straightening and concavity of the pressure curves at $90^0 \geq \alpha \geq 15^0$.

At the same time, according to fig. 83 [3], analogous concavity of the pressure distribution on the plate front side takes place at $\alpha = 6^0$ also. This concavity has a monotonous character and one appears and increases as the attack angle, in the $8^0 \geq \alpha \geq 0$ limits, is increased and, according to it, the velocity head vector is deflected from a normal to the plate profile at its front edge, as it is shown in fig. 6. Visualization of the flow running against the thin plate with its sharp edges at an angle of 2.5^0, adduced in a photo 35 [14], shows quite clearly a striving for separation of the jet stream from the plate front side. Possibility of such separation is prevented by a velocity head pressure of the unrestricted flow outside external boundary of the jet stream. In this connection, the author supposes reasonable to return to a comparison of the well-known question on interaction of the real fluid flow with a thin (infinite thin) plate oriented strictly along the flow. In reality, such plate has a form resistance owing to a presence of viscous boundary layers at its surfaces which ones play a role of a soft obstacle for the flow. Interaction of the flow with such obstacle leads to origin of the weak jet streams creating a rarefaction on both sides of the plate and thereby ones stipulate instability of neutral position of the plate in the uniform flow of the real fluid. As a result of it, the plate is drawn into the oscillatory conditions of a jaw although origin of these oscillations is not bound with initial formation of the vortexes and of its pushing

away from the plate. In this case, the vortexes and the near-wall turbulence are consequence of the plate yaw, but not a cause of its oscillations.

The above-stated description of the conceptual model in combination with the necessary mathematical expressions and graphical constructions is the valuable basis for solution of the problems on interaction of the unrestricted uniform flow of the real fluid with the thin flat plate oriented at any angle of attack.

Fig. 7a shows a constructing of the bifurcation line, BLJ60, of the unrestricted flow part, running immediately against the plate, in a kind of a hyperbola branch for which the plate profile is axis of its symmetry.

Fig. 7b shows a constructing of internal – left and right – boundaries of the jet streams before the plate; the left boundary is constructed, in the beginnings, left out of account a displacement of the bifurcation line, BLJ60, from a middle of the plate profile; the basic flatness line, BFL60, is parallel to the plate profile and one is placed behind it at distance $h_{60} = h_{90} \sin 60^0$ from the latter; asymptotes of these hyperbolas, as internal boundaries of the jet streams, are the central axial (vertical) line and the basic flatness line, BFL60; these hyperbolas pass without fail through the plate edges. And then, the internal boundary of the left jet stream is successively displaced following a displacement of the hyperbolic bifurcation line, BLJ60, from the flow central axis; thereby a constructing of the internal boundaries of the jet streams is completed.

Fig. 7c shows final form of the bifurcation line, BLJ, and internal boundaries of the jet streams.

Fig. 7d shows a constructing of external boundaries of the jet streams before and on both sides the plate; the constructing is carried out in the following way:

- the new - second - basic flatness line, BFL60, is parallel to the first (above-stated), BFL60, and one is placed on a distance equal to $b_{60} = b_{90} \sin 60^0$ from the first BFL60;
- the straight lines passing through the plate edges and parallel to the flow central line are, together with the second BFL60, the new asymptotes of hyperbolic lines on the plate both sides;
- radii $r_{60} = r_{90} \sin 60^0$, at an angle of 45^0 to the flow central axis, are joined to the plate edges;
- the secant parabolas, shown in fig. 3 in the given article, are decreased in its scale proportional to $\sin 60^0$ and ones are joined to the plate edges to be orthogonal to the internal boundaries of the jet streams;
- every of two hyperbolic lines as the external boundary of the jet streams is placed between the new asymptotes and one passes through the free end of the radii orthogonally to the secant parabola respectively.

A quantity of a velocity head of the jet streams is the same that at attack angle of $\alpha = 90^0$, but the force of these jet streams is decreased in proportion to degree of narrowing the unrestricted flow part running immediately against the plate at an attack angle of 60^0, therefore

$$P_{60} = P_{90} \sin 60 = \rho v_0^2 A_{90} \sin 60^0. \quad (7)$$

A degree of rarefaction behind the plate and accordingly intensity of the vortex wake are also decreased in the same proportion.

It should be noted, the displacement of the internal boundary of the left jet stream to the right, following the displacement of the bifurcation line, BLJ, to the right from the plate profile center, leads to adjoining the left internal boundary to the plate front side long before its rear edge and thereby the displacement promotes to a separation of the left jet stream from the plate front side near its rear edge.

Fig. 7d shows also the boundaries of the jet streams after its intersection with the secant parabolas; these boundaries have a kind of elliptical curves, enveloping the flow part – "dead fluid" - behind the plate. It cannot but note the above-described decrease of the jet cross-section ($A_{jp} = A_{j90}/1.08$) and corresponding an increase of the jet velocity ($v_{jp} = 1.08 v_0 \sqrt{2}$) at a line passing through the plate edge and perpendicular to the unrestricted flow direction. These accelerated jet streams involve by turns the dead fluid into the rotary motion and then ones push

by turns against vortexes from the plate down flow; the average in time rarefaction quantity behind the plate is, in this case, $p_{60} = p_{90} \sin 60^0$. Dependence of the rarefaction quantity behind the plate remains in the kind of $p(\alpha) = p_{90} \sin \alpha$ up to $\alpha = 9^0$ when the force - $P_9 = P_{90} \sin 9^0$ – of the every jet stream becomes insufficient for involving by turns the whole of the fluid mass behind the plate into a single large vortex and when the opened hydrodynamic wake in the kind of the vortex street constructed by the large vortexes is changed by the closed wake filled by vortexes with its sufficiently lesser dimensions; a length of the closed wake still exceeds the plate profile width but its length is shortened up to the plate width at $\alpha = 6^0$; later on, the length is shortened up to zero as the attack angle will be decreased up to zero.

A constructing of internal boundary of the jet streams, adduced in fig. 3 ($\alpha = 90^0$) and fig. 7c ($\alpha = 60^0$), quite corresponds to each other, at the same time a constructing of its external boundary has essential difference in the following:

- in the first of these two cases external boundary of the jet streams is constructed by the same way as its internal boundary, i.e. by means of one and the same the basic flatness line, BFL90;
- in the second case external boundary of the jet streams is constructed by means of the new basic flatness line, BFL60, placed on a distance b_{60} from the initial basic flatness line, BFL60.

A cause of such distinction is in that the symmetrical structure of interaction of the flow with the plate, oriented strictly across the flow direction, is essentially simpler than asymmetrical structure of its interaction at the attack angles in $90^0 > \alpha > 0$ the limits. A decrease of the plate attack angle from position $\alpha = 90^0$ is accompanied by separation of the new – intermediate – basic flatness line, BFL, from the initial basic flatness line, BFL90. The new line, BFL, is parallel to the initial line, BFL90, and one moves away from the latter as the attack angle is decreased from $\alpha = 90^0$ up to $\alpha \geq 78^0$, when a distance between these lines will be equal to the width b_{78} of one of these jet streams before the plate. Later on, as the attack angle is decreased, the initial line, BFL90, approaches successively to the plate profile according to dependence $h(\alpha) = h_{90} \sin \alpha$ and one is asymptote for hyperbolical internal boundary of the jet streams, and the new line, BFL, approaches successively initial line, BFL, according to dependence $b(\alpha) = b_{78} \sin \alpha$, and one is asymptote for external boundary of the jet streams. This explanation ensures a constructing of unlimited number of the flow trajectories in the limits of the jet streams and outside its external boundaries at any attack angles of the plate.

Fig. 7e represents a diagram of a constructing of the pressure distribution on the plate front side; the diagram in fig. 7c is here used as a basis of such constructing; it also necessary to take into consideration a preliminary remark: a distinctive feature of the unrestricted uniform flow possessed by a tendency to a motion along the surface of the streamlined body, whereas its pressure acts along the normal to the body surface.

A constructing of the pressure distribution on the plate front side is the following:

- the basic flatness line, BFL60, and the perpendicular to its, passing through an apex of the hyperbola as the bifurcation line, BLJ60, form the asymptotes of two equilateral hyperbolas passing through the plate profile edges; these hyperbolas coincide partially with the internal boundaries of the jet streams close by the basic flatness line, BFL60, and then ones approach the perpendicular to the BFL60;
- these two hyperbolas determine the pressure distribution of the flow on the plate front side by means of the method showed in fig. 2a in previous article of the author [13]; a scale of the pressure distribution is determined by its maximum value equal to ρv_0^2 at the attack angles in the limits of $90^0 \geq \alpha \geq 9^0$ and one is determined by its maximum value equal to $\rho v_0^2 \cos \varphi$ at the attack angles in the $8^0 \geq \alpha \geq 0$ limits.

A separation of the jet stream from the plate front side near its rear edge – the point S, corresponding to fig. 5a – is accompanied by the ejector rarefaction in a clearance between the internal boundary of the jet stream and the plate surface. Rarefaction in the narrow cavity is communicated with rarefaction behind the plate. In a result a part of the plate front side between the separation point, S, and the plate rear edge is found partially unloaded from the flow

pressure. A curve of excessive pressure distribution on the plate intersects smoothly its profile and one is joined with the lateral boundary of the rarefaction zone behind the plate.
The graphical constructing of the boundaries of the jet streams and curves of the flow pressure onto the plate front side at the different attack angles, carried out by the author for himself and not adduced in the given article, allowed to ascertain that the internal boundary of the jet stream at the plate front edge coincides with the flow bifurcation line, BFL15, at $\alpha \leq 15^0$ according to the diagram in fig. 5a at the same time a constructing of external boundary of the same jet stream quite corresponds to the above-stated for the attack angles in the limits of $90^0 \geq \alpha > 15^0$.
Solution stated in two parts of this section of the given article is physically adequate and mathematically sufficiently strict evidence to that the body form induces the jet streams in unrestricted uniform flow of the real fluid. Just the jet streams form the near field in the flow where ones determine both kinematics of the flow and dynamics of interaction of the flow with the body. Just the jet streams determine the body form resistance as the so-called drag. Just the jet streams determine kinematics and dynamics of the far field of the flow. At the same time just the real fluid viscosity masks the outside and inside boundaries of the jet streams with the passing flow parts surrounding its.
3. This part of the solution is completely based on the methodology and the results stated in previous two parts and one is intended only for explanation of the question: why these jet streams cannot be seen in the numerous photos of the corresponding visualized flows. The answer is the following:
- halve a width of one of two jet streams, before the plate, by a straight line parallel to the flow central line; halve the radius, $r_{90}(\alpha)$, of external boundary of the jet stream according to it;
- draw a straight line parallel to the initial basic flatness line, BFL60, on a distance from it equal to the half-width of the same jet stream before the plate;
- these two crossing lines are asymptotes of a hyperbola as an intermediate trajectory of the flow between the internal and external boundaries of the jet stream;
- construct the hyperbola using the linear interpolation between hyperbolas as the internal and external boundaries of the jet stream and at the same time keeping its orthogonal intersection with the secant parabola arch;
- supplement the hyperbola with the inverse curvature parabola arch after intersection the hyperbola with the secant parabola;
- reiterate similar constructing in the intervals between the jet stream boundaries and the above construction;
- reiterate similar constructing beyond the external boundary of the jet stream.
Figs. 8, 9 show the examples of such constructing.
Such constructing allows taking sufficiently uniform field of the flow trajectories of the elementary jet streams of the real fluid flow. This field shows a smooth degeneration of a curvature of the flow trajectories and a corresponding decrease of the heightened velocity near the plate edges up to its rated quantity far from the plate.
Such field of the flow trajectories corresponds quite to the results of visualization taken by means of experiments. But even in such presentation, it cannot be notice a zone of the most intensive increase of the flow velocity near the plate edge. The boundaries of this zone and the velocity average quantity in it have been described in previous two parts of the solution. Such simplified approach is justified by that the most part of hydraulic losses in it stipulated in the main by the flow acceleration near the plate edges has been taken into account.

Discussion of results
The given problem, by its statement of the question, corresponds to a notion of the direct problem since its solution is directed onto elucidation of a distribution and quantity of the forces acting in concrete system of interaction of the body and the fluid flow at the given quantity and the given direction of a potential difference of the motive force applied to the interaction system.

From this point of a view J. Kepler – I. Newton problem is the inverse problem since its kinematic and dynamic analysis of the interaction system is directed onto determination of the motive force applied to the interaction system.
Such comparison of the problems is not bound with a vainglorious aspiration of the given article author but it is stipulated by the method of its solution:
- in the inverse problem, a use of the curves from assemblage of conical sections – an ellipse, a parabola, a hyperbola – taken separately each other as the trajectories of the heavenly bodies allowed Kepler to establish the three laws of kinematics of the solar system planets and then the kinematic basis allowed to determine the motive force of the system in a kind of the single Newton's law of universal gravitation;
- a use in the direct problem of the same curves in its orthogonal conjugation allowed to solve the problem of the flow kinematics in the kind of the graphic-analytical reproduction of a field of the flow trajectories of the real continuous medium around the obstacle, and then on this basis one allowed to determine the distribution and quantity of its interaction forces.
In a 100 years from publication of Newton work [1], Du Buat, in the preface to the second edition of his two-volume monograph [15], describing the hydromechanics state, was marking "the inexact acknowledgement of the science principles, erroneous theories disproved by experiment, scarcity of observations made up to now and difficulty of its realization". Approximately in the middle of XX century, G.D. Birkhoff [7] marked in jest: the ones are observing the inexplicable while others are explaining the unobservable. In spite of a humorous shade, the expression stands in need of settlement.
The first part of the above-stated solution is realized by means of the simplest case of an interaction of the unrestricted flow with the thin flat plate submerged strictly across the flow and therefore the solution is a matter principle for understanding of the main point. The solution part elucidates a possibility of transformation of the uniform flow into the jet streams before the obstacle which ones pass around the obstacle and thereby ones create two types of the power influence upon the obstacle: the heightened pressure onto the obstacle front side and a rarefaction zone behind the obstacle; such power influence determines all dynamics of interaction of the flow and the obstacle. The internal boundaries of the jet streams determine the flow pressure onto the body front side; the external boundaries of the jet streams together with its internal boundaries determine an intensity of the ejector action behind the body; at the same time both these boundaries are the flow trajectories.
The second part of the solution shows a change of the parameters of the flow initial structure accordingly to a change of the attack angle of the plate and one shows also the partial separation of the pressure lines from the internal boundaries of the jet streams as the flow trajectories; in the first part of the solution these lines were completely coinciding; a conservation of the initial structure of the flow field and at the same time a change of its parameters show a community of the solution achieved in the first part.
This third part of the solution shows a harmonious compatibility of the boundaries of the jet streams with the flow trajectories in the near and far fields; such harmonious compatibility creates an illusion of the uniform diminution of curvature of the flow trajectories as ones move away from the body. But the fact is the average quantities of the curvature and compactness of the flow trajectories in the near flow field are quite visibly differ from those in the far flow field.
The solution clears the way of its further development for determination of the interaction kinematics and dynamics of the unrestricted real fluid flow with the plate of the finite span. The new solution will be bound not only with the concentric large-vortex structures behind the plate but also with the helical vortex structures accompanying an interaction of the jet streams with the mentioned concentric vortexes near the plate ends and also with degeneration of the large-vortex structures and with a corresponding decrease of rarefaction behind the plate as its span is decreased up to the unit length.
The results of experimental determination of the plate drag coefficient of its infinite and finite span, adduced by Prandtl in his monograph [4], allow to ascertain that the notion on the plate

infinite span corresponds to a ratio of the plate length to its width no less than 50 times; at such and greater relative length of the plate its drag coefficient is ~ 2.0. Another utmost case is realized by equality of the plate length to its width in the kind of the square plate. Its drag coefficient by Prandtl is 1.10, and the quantity corresponds very closely to the circular plate drag coefficient: from 1.10 to 1.12. The expressions (6a, b), in the given article, allow to determine a quantity of the drag coefficient component stipulated by rarefaction behind the square plate

$$C_D = \pi/4 + x = 1.10, \quad (8)$$

whence it follows: $x = 0.3146$ ....
According to the expression (5) the drag coefficient component of the infinite span plate is $1/\sqrt{2} = 0.7071$ ..., i.e. that component is in ~2.25 times as much. This simple calculation, in the author opinion, evidence to that a decrease of the plate relative span from its 50-times quantity is accompanied, in the beginning, by a corresponding decrease of a zone behind the plate, filled by the concentric large-vortex structure; when the plate span and its width become commensurable and then become equal to each other, the jet streams envelop more or lesser uniformly the plate perimeter and ones discontinue a formation of the large-vortex structure behind the plate; accordingly to it, the rarefaction degree behind the plate is decreased in ~2.25 times.
In general, it is ascertained phenomenon of formation of the jet streams in the unrestricted uniform flow of the real fluid induced by an obstacle on the flow way.
The near field contains the jet streams streamlining immediately the obstacle and ones, at the same time, ensure, in the main, fulfillment of the flow continuity condition.
Internal boundaries of the jet streams determine not only effective trajectories of the immediate passing round of the obstacle but ones allow constructing the flow pressure profile onto the obstacle front side.
A condition of interaction of the flow with the obstacle surface has been elucidated in the kind of the rule: the real fluid flow strives for a motion along the obstacle surface, at the same time the fluid pressure acts along a normal to the obstacle surface. The jet streams envelop the fluid zone behind the obstacle and ones exert the ejector action onto the fluid.
Characteristic trajectories and the pressure profiles, determining the plate drag at any angles of attack, are constructed in the kind of orthogonal conjugation of curves from assemblage of conical sections for the simplest case of interaction of the unrestricted uniform flow of real fluid with the flat plate of infinite span.
In that way the nature of the body form resistance has been elucidated, and the conception, in combination with the boundary layer theory, creates theoretical prerequisites for solution of other interior and exterior problems of aero- and hydromechanics at axial symmetrical, two- and three-dimensional statement.

Final remarks
Here are three solved problems:
1. The problem on a contactless – field - interaction of two real solid bodies of the simplest form – sphere (ball) – under action of gravitational force at the free space [1]. Spatial differentiation of the motion trajectories of the bodies is described by the separate lines from assemblage of conical sections.
2. The problem on a contact interaction of real continuous fluid, moving uniformly and rectilinearly under action of a given pressure difference, with the body of the simplest form – the flat plate of infinite span (solved here). The interaction induces the spatial differentiation of the fluid flow in the kind of the near and far fields around the obstacle. A profile of the flow trajectories is described by orthogonal conjugation of the lines from assemblage of conical sections.
3. The problem on intra-contact interaction of a body of the simplest form – the right circular cylinder – from the isotropic elastic-plastic material under action of longitudinal tension [16].

The action induces spatial differentiation of the stressed state of the body continuous material and leads to formation of the body core and casing parts. As a result of interaction of these parts at the tension successive increase, the body form, in the beginning, takes the shape of the hardly noticeable rotary hyperboloid; and immediately before the body elastic failure, the body form change is additionally accompanied by a formation of a local narrowing – so called neck – in the kind of the right hyperboloid surface of rotation and two evolventoid of rotation with its inverse curvature, conjugating smoothly the hyperboloid with the body rest surface.
In that way the curves from assemblage of conical sections discovered ~ 2400 years ago are finding its applications during the last ~ 400 years in the fields, in the beginning, in celestial mechanics, then in mechanics of rigid body [16] and now in the fluid mechanics.

Acknowledgements
Author wants to express his deep gratitude to his son Alexey for the computer carrying out of the article and his daughter Catherine for her caring for her father.

---

[1] I. Newton, Philosophiae naturalis principia mathematica, London, 1687 – Transl. from Latin into Rus., with commentary and notes by A.N. Krilov, Complete works, Vol. 7, Moscow – Leningrad, 1936
[2] L.M. Krivonosov, Y.S. Stoljarov, Riddles of blue ways, Education State Publishing, 1967
[3] H. Lamb, Treatise on the Mathematical Theory of the Motion of Fluids, 6th Ed., 1932 – Hydrodynamics – Transl. from Engl. into Rus., State Publishing of Technical and Theoretical Literature, Moscow – Leningrad, 1947
[4] L. Prandtl, Fuhrer durch die stromunglehre, 2nd Ed., Gettingen, 1944 – Hydroaeromechanics – Transl. from Germ. into Rus., Foreign Literature State Publishing, Moscow, 1949
[5] H. Schlichting, Grenzschicht theorie, 5th Ed., Verlag G. Braun, Karlsruhe, 1965 – The boundary layer theory – Transl. from Germ. into Rus., Nauka State Publishing, Moscow, 1969
[6] D. Meksyn, New Methods in Laminar Boundary-Layer Theory, Pergamon Press, N.Y., 1961, pp. 15 and 109
[7] N.V. Kokshaysky, Essay on biological aero- and hydrodynamics (flight and swimming of animals), Nauka State Publishing, Moscow, 1974
[8] S. Goldstein, Modern developments in fluid dynamics, 2nd Ed, Vol. 1, 1943 – Transl. from Engl. into Rus., Foreign Literature State Publishing, Moscow, 1948
[9] M.I. Gurevitch, Theory of jets of ideal liquid, Physical and Mathematical Literature State Publishing, Moscow, 1961
[10] M.A. Lavrentjev and B.V. Shabat, Problems in hydrodynamics and its mathematical models, 2nd Ed., Nauka State Publishing, Moscow, 1977
[11] M.V. Morkovin, Flow Around Circular Cylinder – a Kaleidoscope of Challenging Fluid Phenomena, in: P.K. Chang, Separation of Flow, Pergamon Press, Oxford, 1970 – Separated Flows – Transl. from Engl. into Rus., Vol. 1, Mir State Publishing, Moscow, 1972
[12] S.M. Bjelotserkovsky, V.N. Kotovsky, M.I. Nisht, R.M. Fjodorov, The mathematical simulation of the flat-parallel separated flow around body, Ed. by S.M. Bjelotserkovsky, Nauka State Publishing, Moscow, 1988
[13] S.L. Arsenjev, The fluid motion physics: The interaction mechanics of a free liquid jet with a body and with the other free liquid jet, http://uk.arXiv.org/abs/physics/0801.4160, 2008
[14] M.D. Van Dyke, An Album of Fluid Motion, The Parabolic Press, Stanford, CA, 1982 – Transl. from Engl. into Rus., Mir State Publishing, Moscow, 1986
[15] A.K. Biswas, History of hydrology, Amsterdam - London, 1970 – Transl. from Engl. into Rus., Man and water, Hydrometeoisdat State Publishing, Leningrad, 1975
[16] S.L. Arsenjev, To the Strength First Problem Solution: Mechanics of a Necking, http://uk.arXiv.org/abs/physics/0609149, 2006

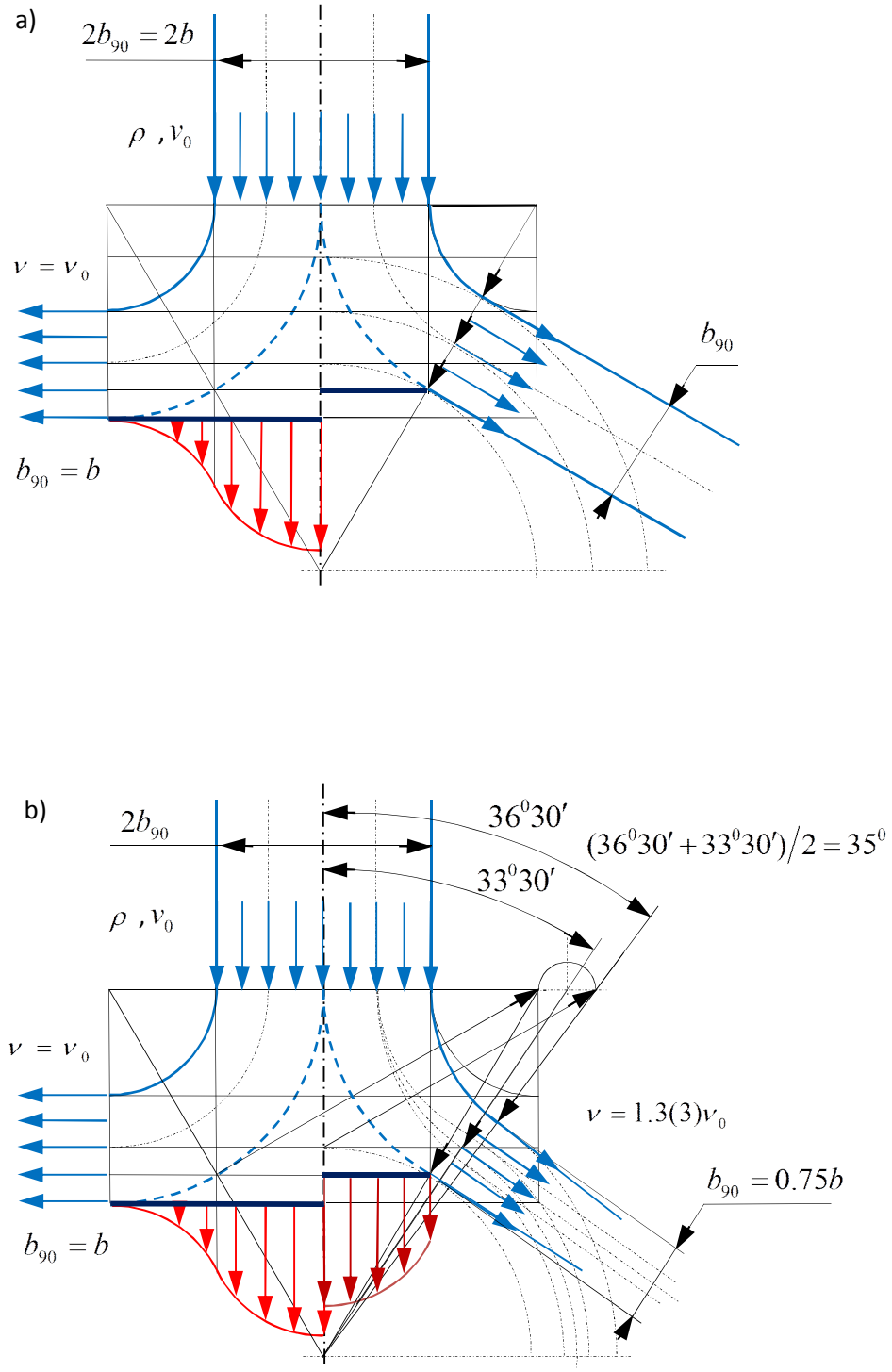

Fig.1. The right side of diagram, a), is the simplest – unreal – constructing of trajectory of a free flat liquid jet running against a flat plate when the plate width and the jet thickness are equal; the right side of diagram, b), is a constructing of the trajectory – other things being equal – with due regard for an edge effect; the left side of the diagrams is adopted from [13, fig. 2a]

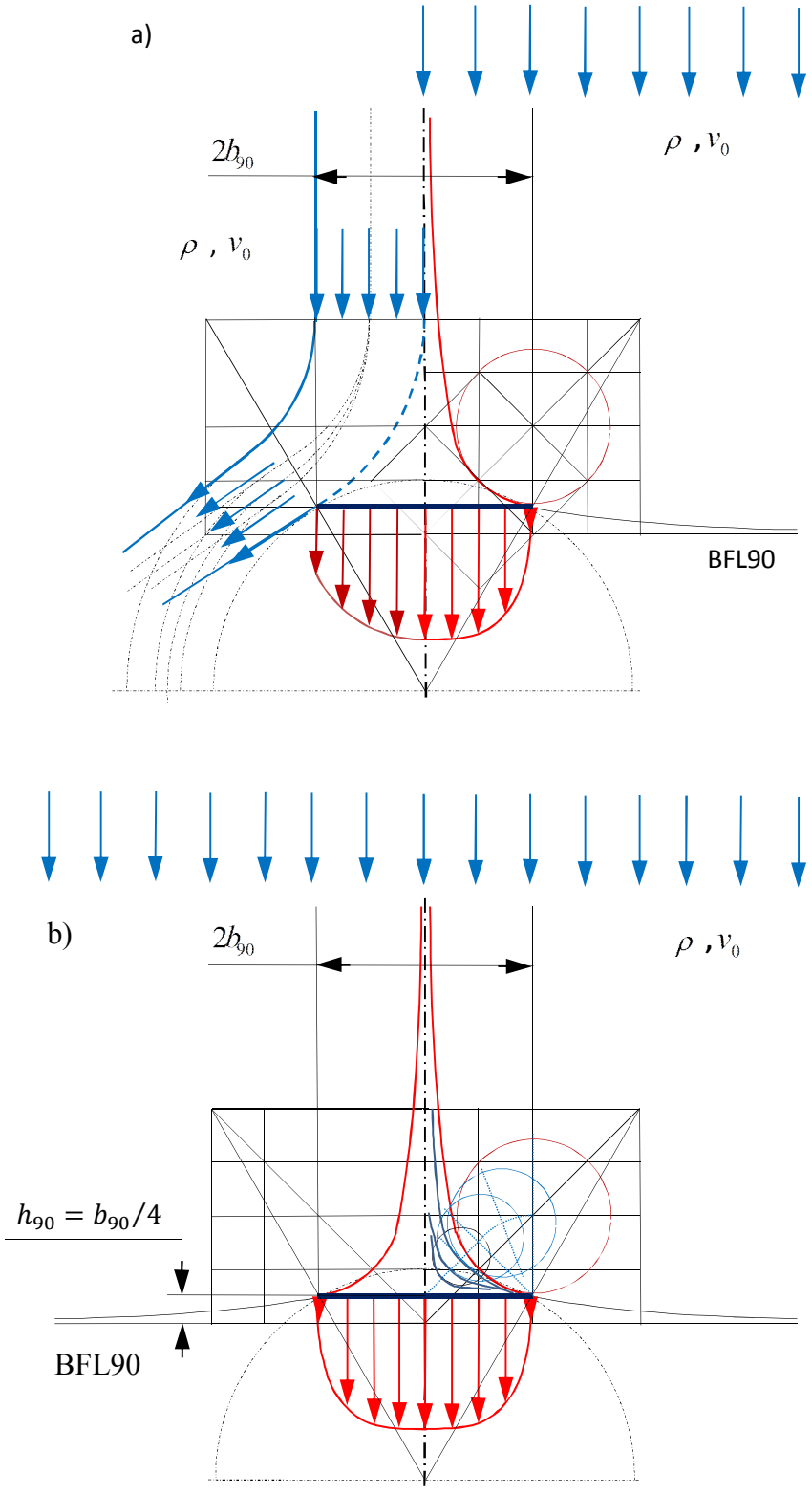

Fig.2. The right side of diagram, a), is a constructing of hyperbolic effective internal boundary of the jet stream formed by the flat plate in the unrestricted air flow; the right side of diagram, b), is a constructing of the flow lines in the braking zone of the flow before the plate

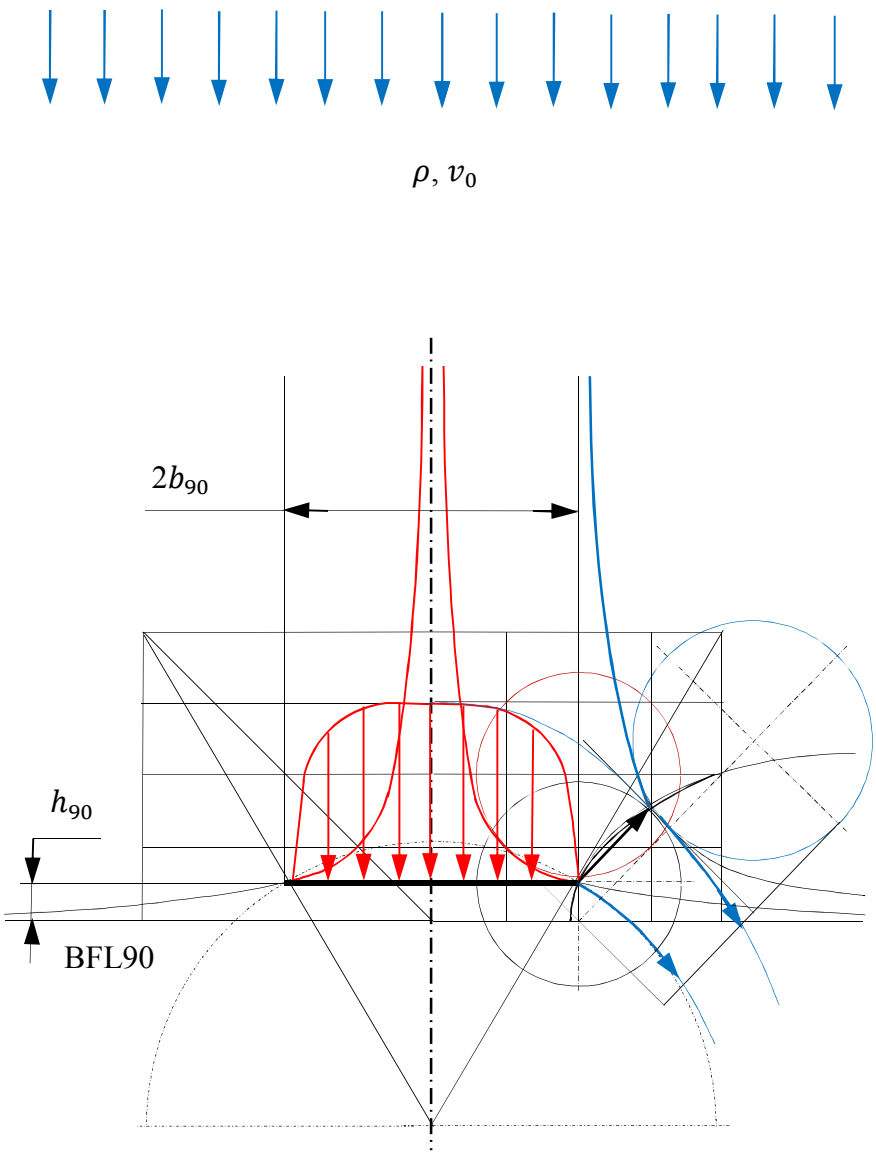

Fig.3. The right side of diagram is a constructing of hyperbolic effective external boundary of the jet stream formed by the flat plate in the unrestricted air flow

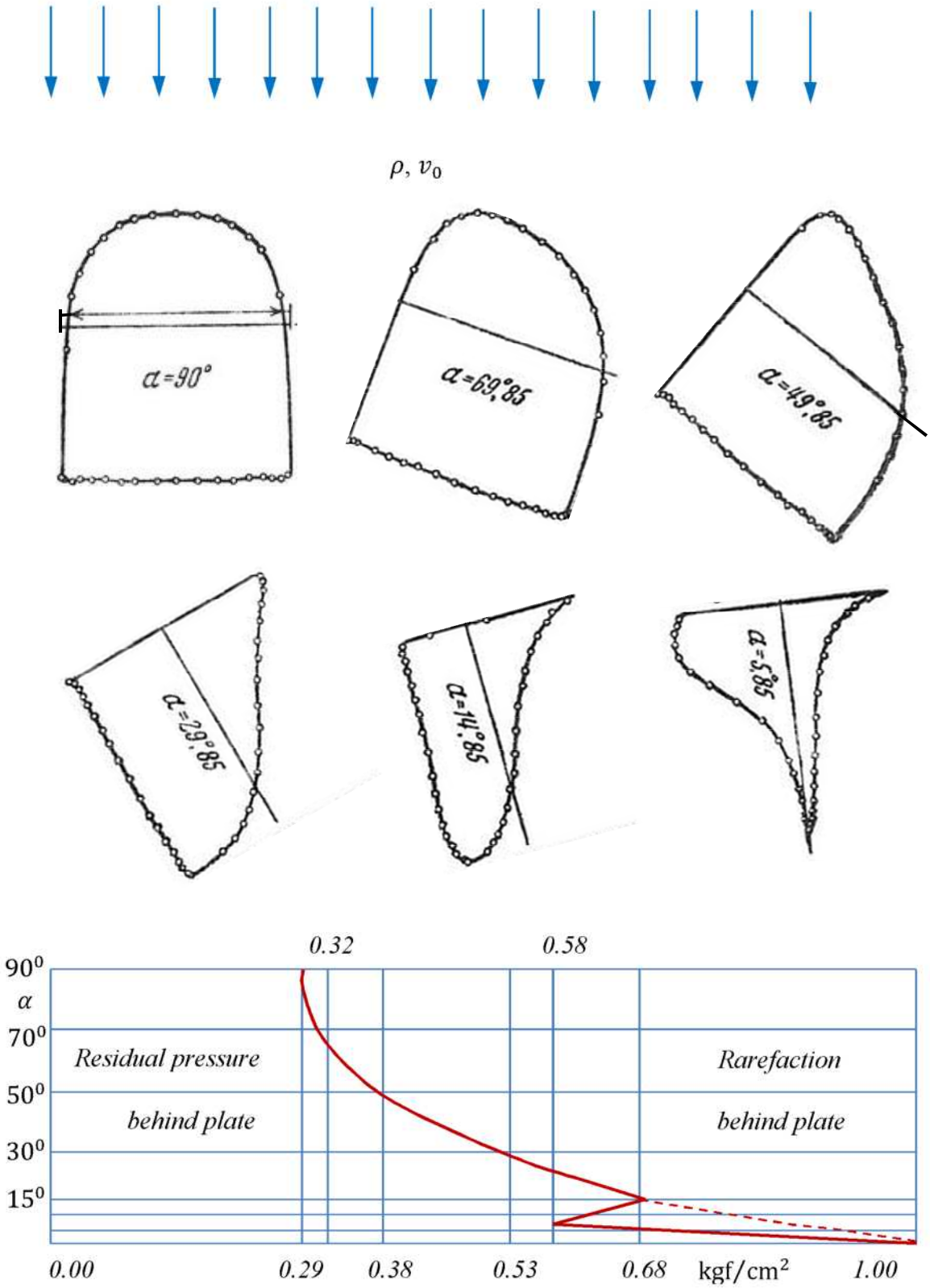

Fig.4. The upper part is the series of diagrams adopted from [3, fig. 83] and presented in its physically natural positions; the lower part is a dependence of rarefaction (as average in time quantity) behind the plate at its attack angles according also to [3, fig. 83]

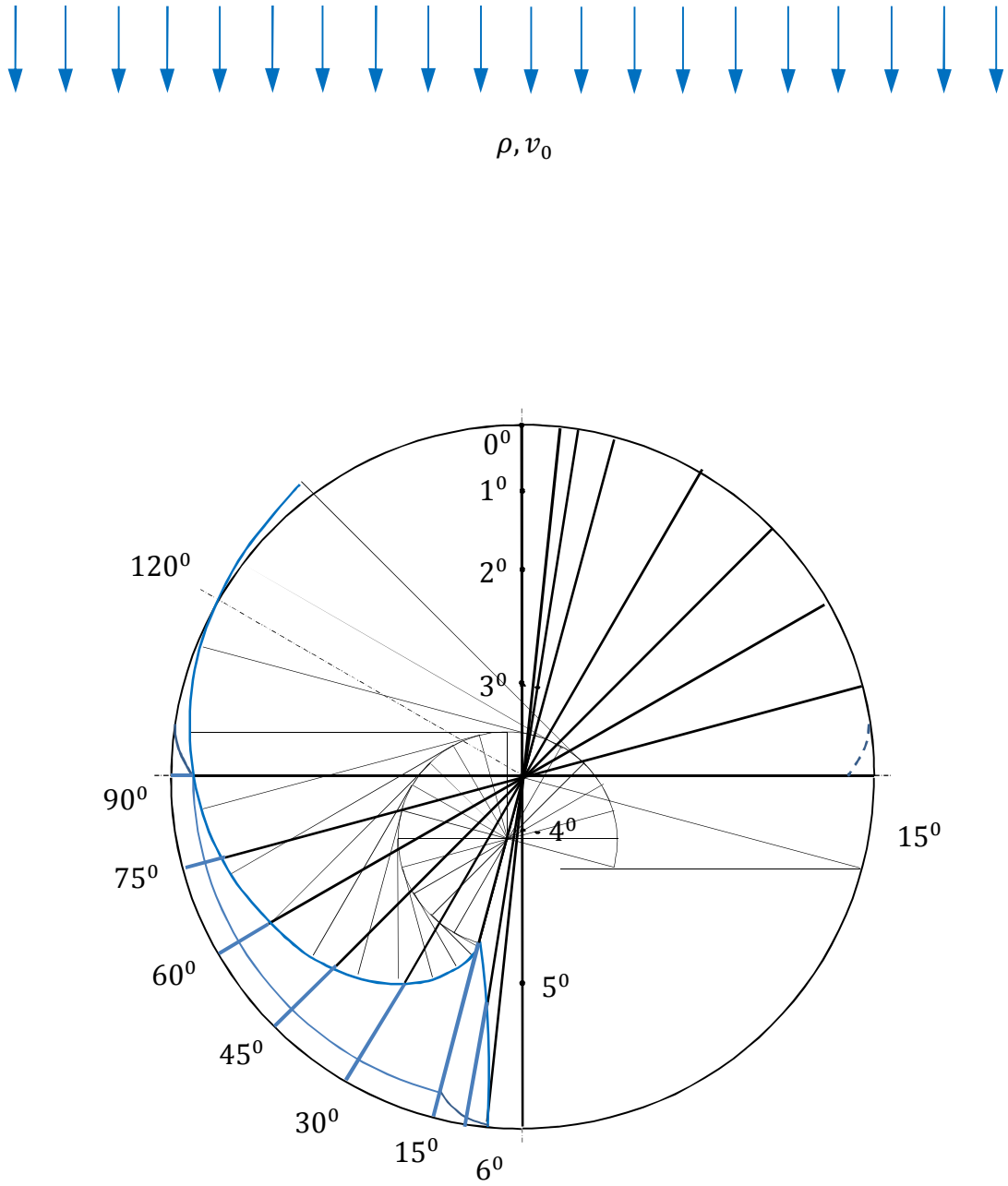

Fig.5a. The circumference evolvent indicates a length of the separation zone of internal boundary of the jet stream from the plate front side near its rear edge at $90^0 \geq \alpha \geq 15^0$ attack angles

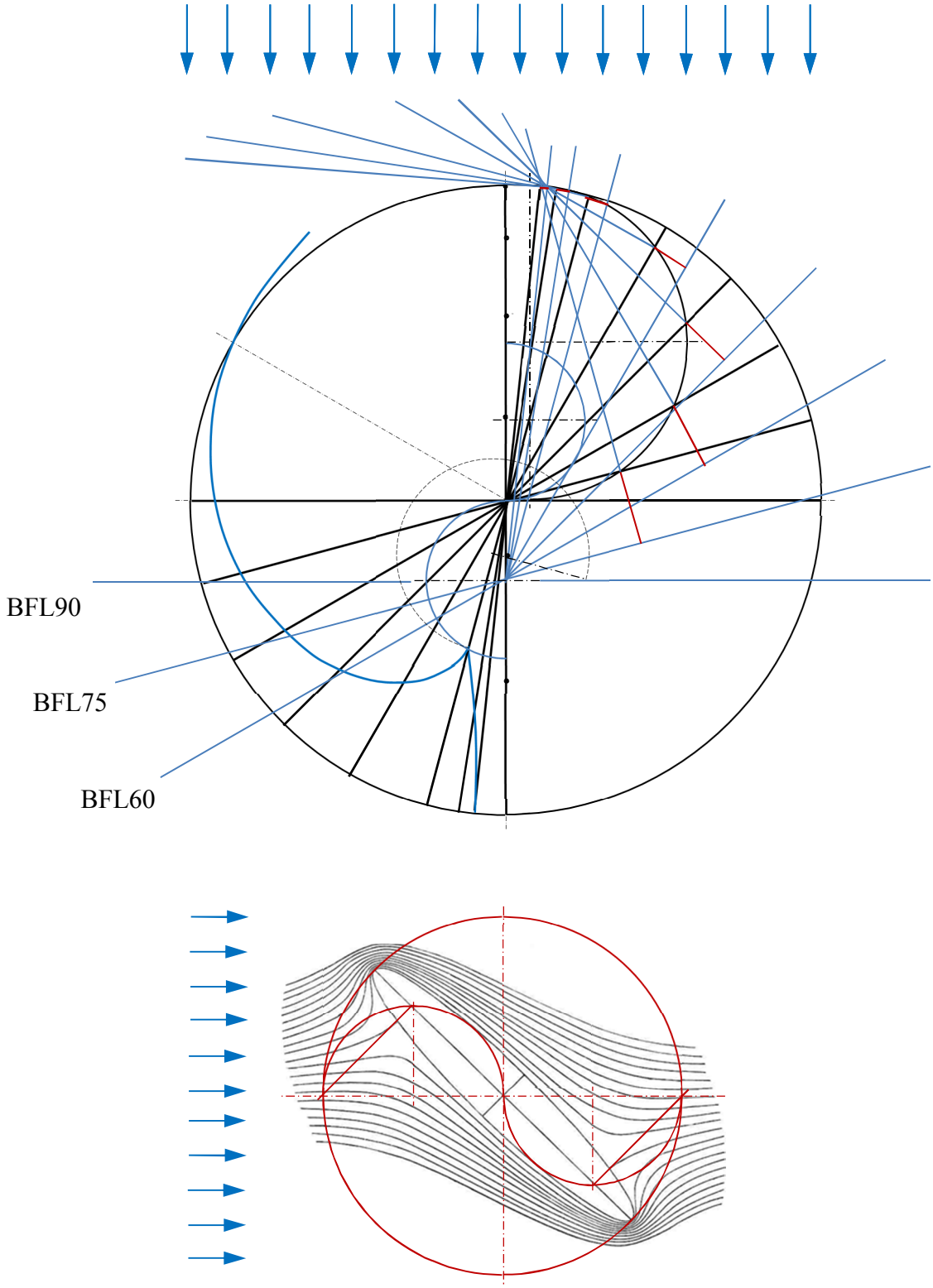

Fig.5b. The intersection point of semi-circumference, displaced to the right from the flow central line, with the plate profile indicates deflection of the bifurcation line, BLJ, from the flow central line; the basic flatness lines, BFL, and normal to its are also constructed here; a diagram, placed below, is constructed on the basis of fig. 34 in [8] for ideal fluid

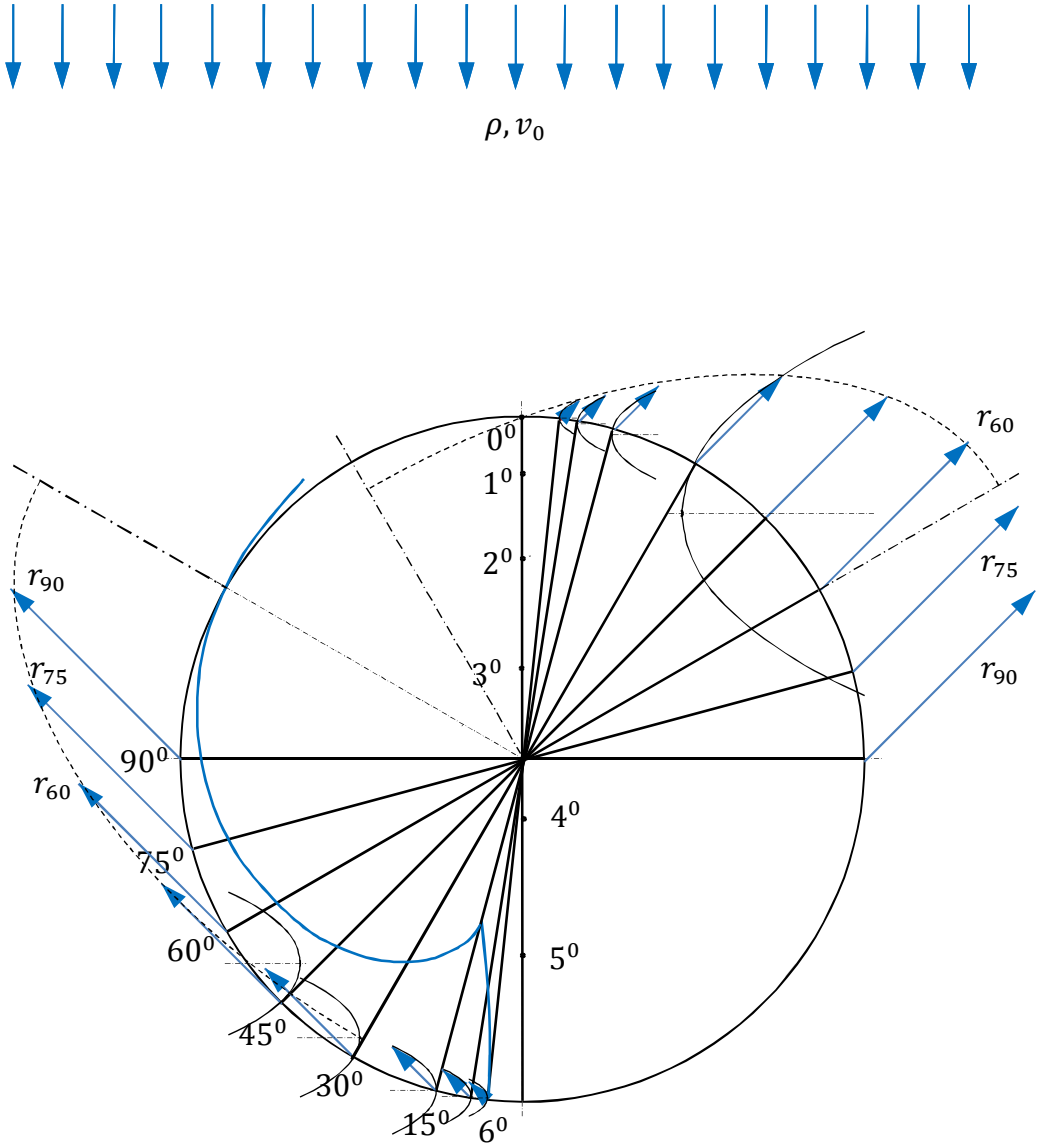

Fig.5c. A constructing of the radii and secant parabolas at the plate edges

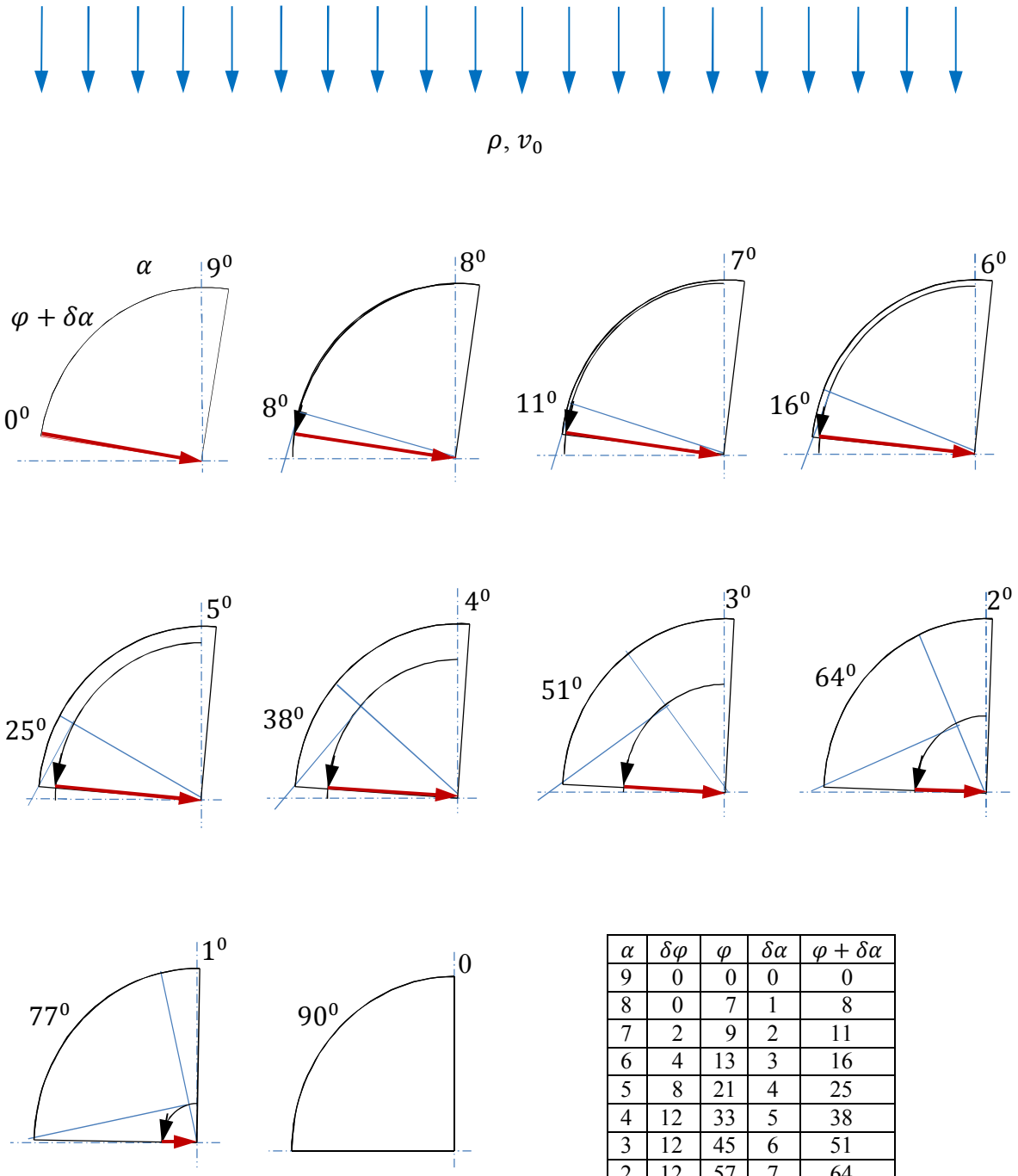

α	$\delta\varphi$	φ	$\delta\alpha$	$\varphi + \delta\alpha$
9	0	0	0	0
8	0	7	1	8
7	2	9	2	11
6	4	13	3	16
5	8	21	4	25
4	12	33	5	38
3	12	45	6	51
2	12	57	7	64
1	12	69	8	77
0	12	81	9	90

Fig.6. Series of diagrams shows a diminution of the maximum velocity head applied to the plate front edge as the attack angle is decreased in $9^0 \geq \alpha \geq 0$ the limits

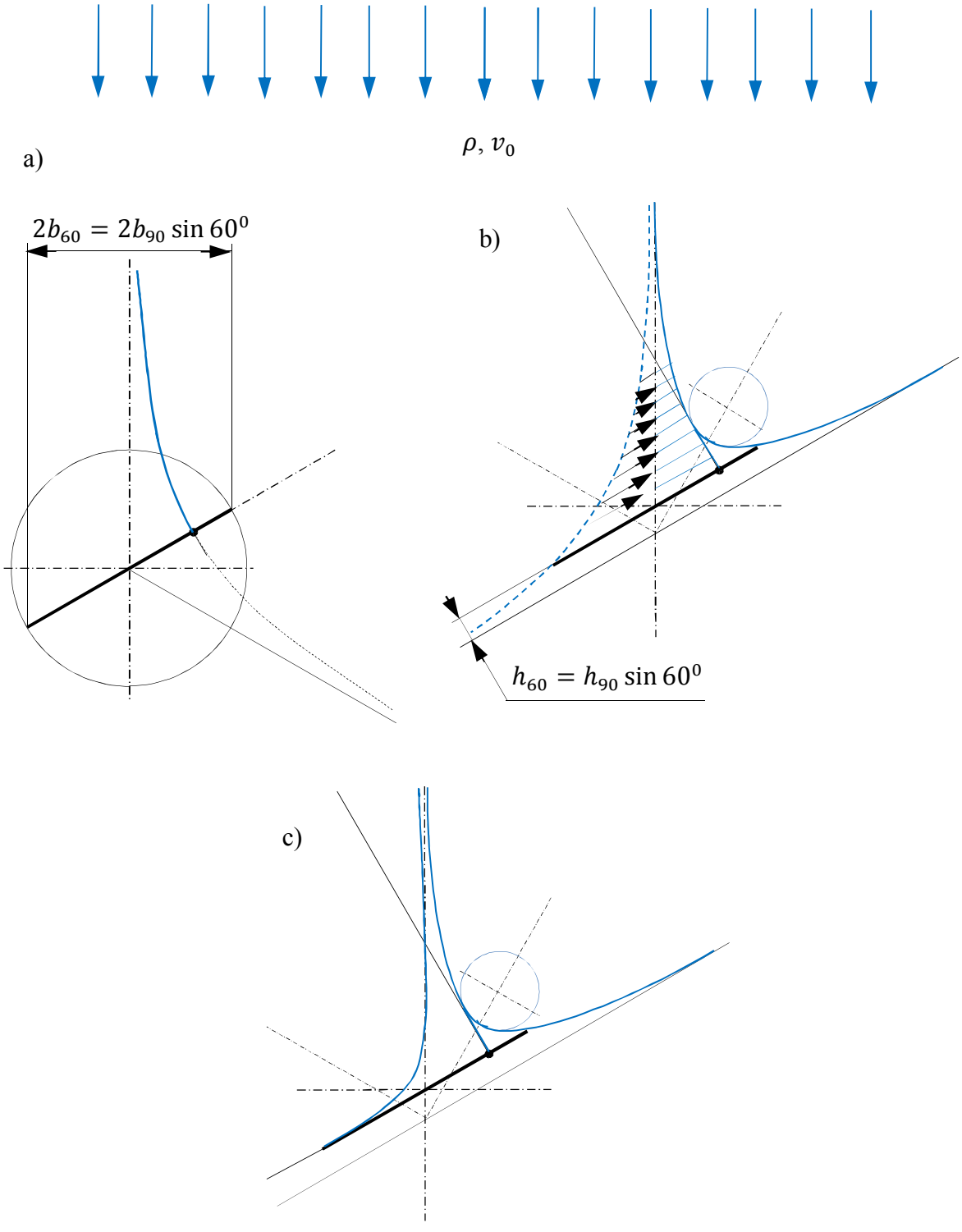

Fig.7a. Preliminary construction of the bifurcation line, BLJ60, of the unrestricted flow part running immediately against the plate at 60^0 attack angle
Fig.7b. A constructing of internal boundaries of the jet streams before the plate; a final form of the left internal boundary is reached by its displacement following a deflection of a final form of the bifurcation line, BLJ60, from the flow central line
Fig.7c. Final form of internal boundaries of the jet streams before the plate front side

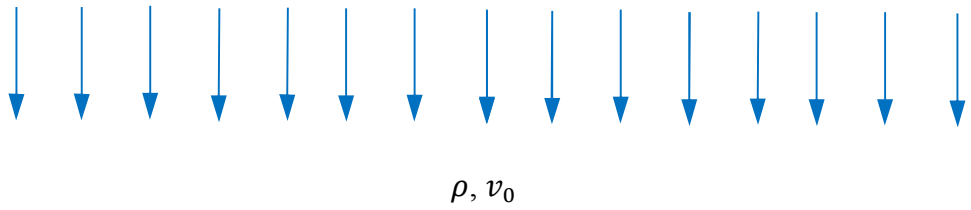

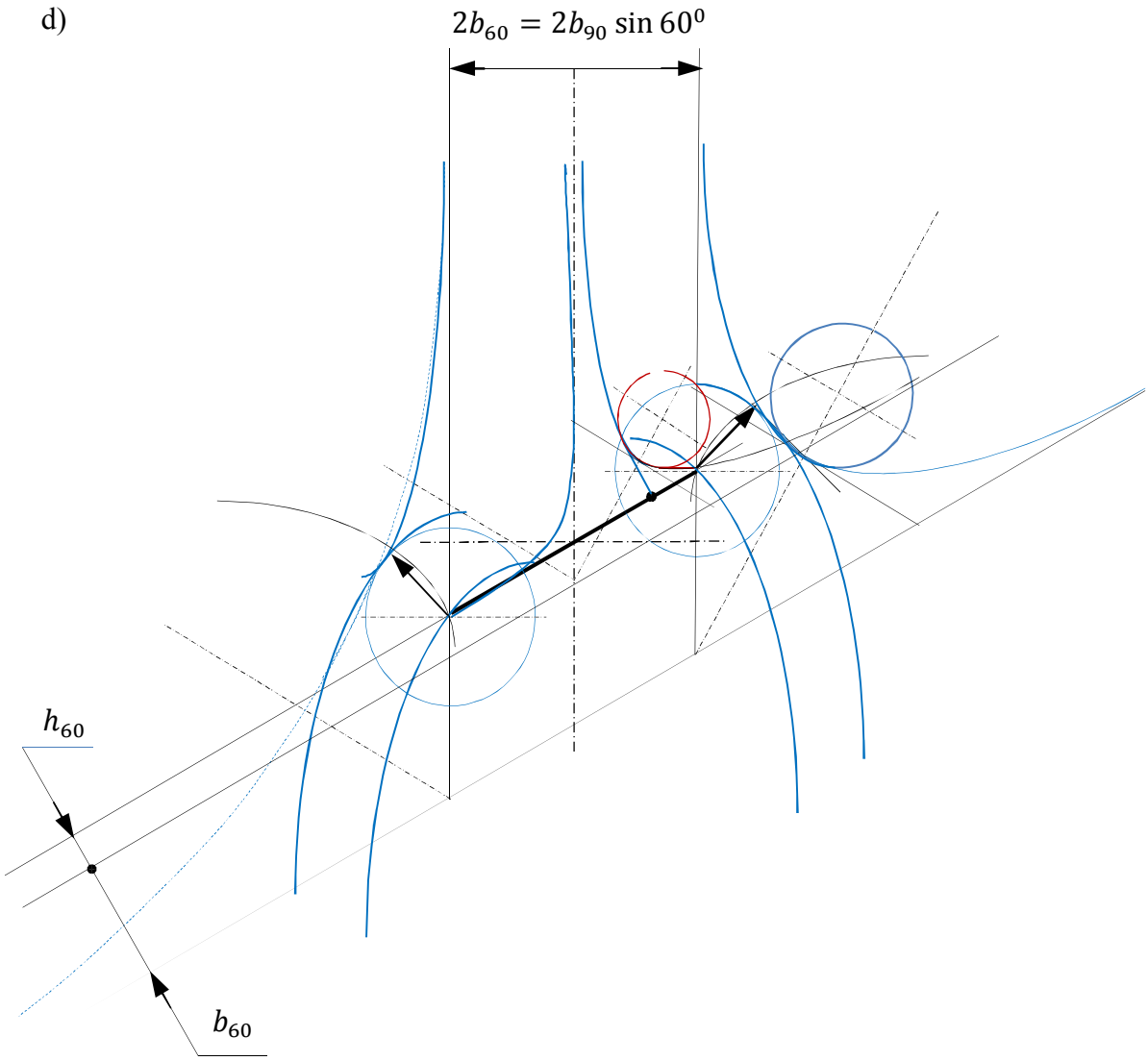

Fig.7d. A constructing of external boundaries of the jet streams by means of a new – second – basic flatness line, BFL60, radius r_{60} and the secant parabolas decreased in its scale in proportion to $\sin 60^0$

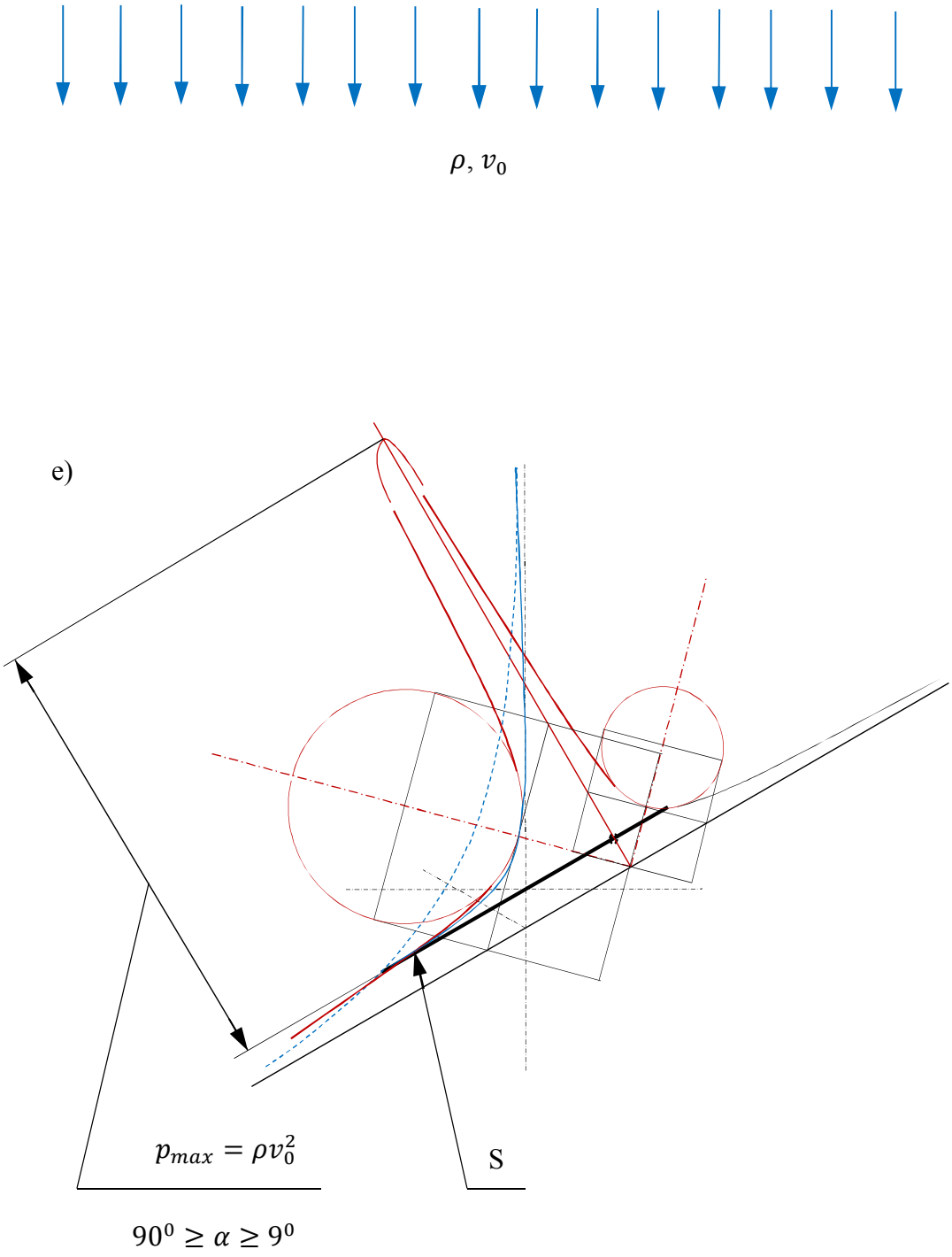

Fig.7e. Diagram for determination of the pressure profile on the plate front side

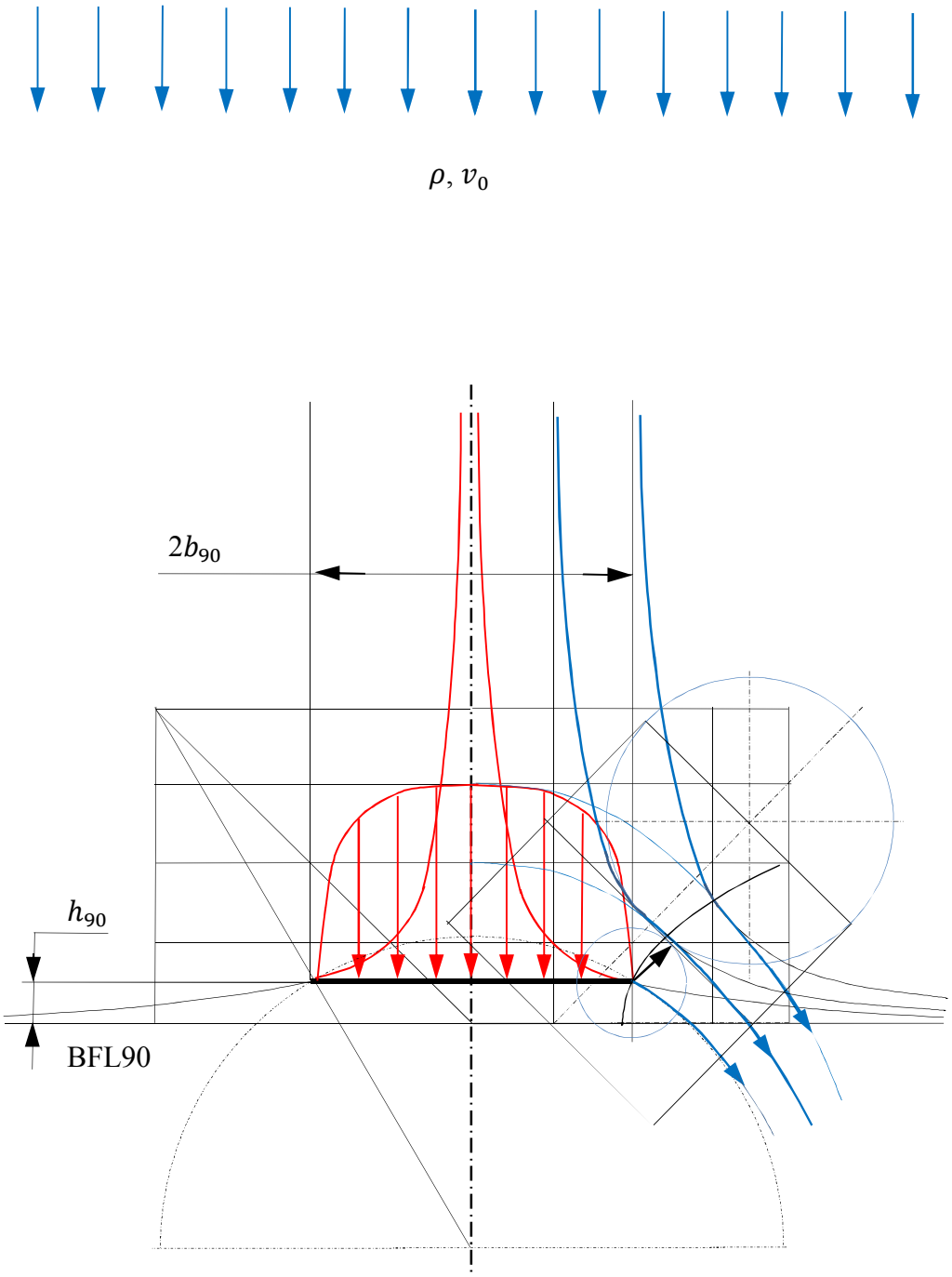

Fig.8. Example of a constructing of the flow intermediate trajectory in the jet stream limits

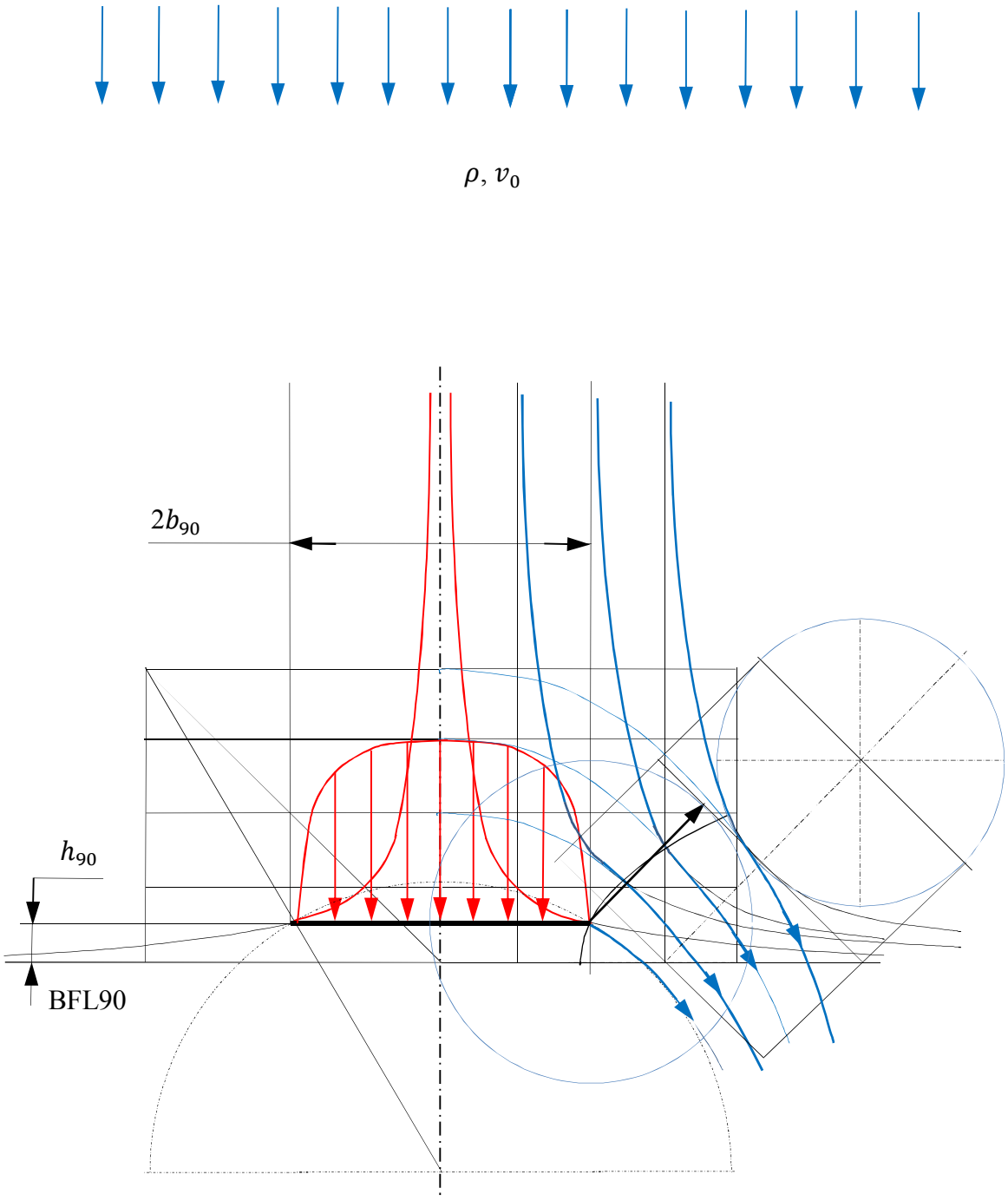

Fig.9. Example of a constructing of the flow intermediate trajectory outside the jet stream